ALLAN DE MARCOS LAPAZ

SELENIUM AS A MITIGATOR OF IRON DEFICIENCY IN SOYBEANS

Thesis submitted to the Plant Physiology Graduate Program of the Universidade Federal de Viçosa in partial fulfillment of the requirements for the degree of *Doctor Scientiae*.

Adviser: Prof. Dr. Cleberson Ribeiro

Co-adviser: Prof. Dr. Maximiller Dal-Bianco Lamas Costa

VIÇOSA
MINAS GERAIS – BRAZIL
2024

Ficha catalográfica elaborada pela Biblioteca Central da Universidade Federal de Viçosa - Campus Viçosa

T
L299s
2024

Lapaz, Allan de Marcos, 1987-
Selenium as a mitigation of iron deficiency in soybeans / Allan de Marcos Lapaz. – Viçosa, MG, 2024.
1 tese eletrônica (67 f.): il. (algumas color.).

Texto em português e inglês.
Inclui apêndice.
Orientador: Cleberson Ribeiro.
Tese (doutorado) - Universidade Federal de Viçosa, Departamento de Biologia Vegetal, 2024.
Inclui bibliografia.
DOI: https://doi.org/10.47328/ufvbbt.2024.272
Modo de acesso: World Wide Web.

1. Soja - Crescimento. 2. Antioxidantes. 3. Micronutrientes. 4. Fotossíntese. 5. Soja - Metabolismo. 6. Selênio. 7. Soja - Efeito do ferro. I. Ribeiro, Cleberson, 1980-. II. Universidade Federal de Viçosa. Departamento de Biologia Vegetal. Programa de Pós-Graduação em Fisiologia Vegetal. III. Título.

CDD 22. ed. 633.34

Bibliotecário(a) responsável: Bruna Silva CRB-6/2552

ALLAN DE MARCOS LAPAZ

SELENIUM AS A MITIGATION OF IRON DEFICIENCY IN SOYBEANS

Thesis submitted to the Plant Physiology Graduate Program of the Universidade Federal de Viçosa in partial fulfillment of the requirements for the degree of *Doctor Scientiae*.

Approved: February 21th, 2024.

Assent:

Documento assinado digitalmente
gov.br
ALLAN DE MARCOS LAPAZ
Data: 10/07/2024 16:03:08-0300
Verifique em https://validar.iti.gov.br

Allan de Marcos Lapaz
Author

Documento assinado digitalmente
gov.br
CLEBERSON RIBEIRO
Data: 10/07/2024 18:28:50-0300
Verifique em https://validar.iti.gov.br

Prof. Dr. Cleberson Ribeiro
Adviser

ACKNOWLEDGEMENTS

To the Federal University of Viçosa, for providing the opportunity to complete this postgraduate course.

This study was partially financed by the Coordenação de Aperfeiçoamento de Pessoal de Nível Superior – Brasil (CAPES) – Finance Code 001.

To my parents, Marcos Antônio Lapaz and Maria de Fatima Rosseto, and my fiancée, Camila Hatsu Pereira Yoshida, for their support throughout this journey.

To my advisor, Prof. Dr. Cleberson Ribeiro, and my co-advisor, Prof. Dr. Maximiller Dal-Bianco, for their technical knowledge and trust in me.

To all my friends from the Agronomy undergraduate program and the Plant Physiology graduate program.

RESUMO

LAPAZ, Allan de Marcos, D.Sc., Universidade Federal de Viçosa, Fevereiro de 2024. **Selênio como mitigação da deficiência de ferro em soja**. Orientador: Cleberson Ribeiro. Coorientador: Maximiller Dal-Bianco Lamas Costa.

Embora o ferro (Fe) seja abundante na maioria dos solos agrícolas, sua biodisponibilidade para as plantas é limitada. A deficiência de Fe pode causar alterações significativas nos metabólitos vegetais, impactando o ciclo de vida da planta. Neste contexto, o selênio (Se) tem demonstrado efeitos promissores contra a deficiência de Fe. No primeiro experimento, avaliamos o possível efeito benéfico do Se aplicado na solução nutritiva sobre pigmentos fotossintéticos, estado nutricional, acúmulo de espécies reativas de oxigênio, metabólitos de ascorbato e glutationa, atividade de enzimas envolvidas na via de síntese desses metabólitos e enzimas de defesa antioxidante, incluindo expressão de isoformas de superóxido dismutase (SOD), após exposição à ausência, deficiência e suficiência de Fe em combinação com ausência e presença de Se. A maior remobilização de Fe associada à manutenção da concentração foliar de N resultou na mitigação da clorose foliar e diminuição da perda de pigmentos fotossintéticos na ausência de Fe com Se. Adicionalmente, sob essa condição de cultivo, o principal efeito positivo do Se mostrou associado à modulação do ciclo da glutationa. O fornecimento de Se também reduziu a necessidade de substituição de SOD-Fe por SOD-Cu devido à modulação positiva na interação entre Fe e Cu, bem como atenuou o desequilíbrio nutricional de Zn e Mn, principalmente na ausência de Fe. Esses ajustes impediram a peroxidação lipídica em plantas tratadas com Se. No segundo experimento, avaliamos os efeitos do Se sobre a massa seca, concentração de Fe nas raízes e na parte aérea, bem como avaliamos o desempenho fotossintético e o metabolismo primário em plantas de soja submetidas à deficiência de Fe. Na ausência de Fe, as plantas tratadas com Se exibiram modulação positiva na taxa de assimilação líquida de CO_2, melhorando a eficiência de carboxilação e as características fotoquímicas em comparação às plantas sem Se. A ausência sinérgica de Se e Fe comprometeu a massa seca da parte aérea e da raiz e a concentração de proteína. Portanto, essas descobertas destacam o potencial do Se como uma intervenção valiosa para mitigar a deficiência de Fe em culturas de soja.

Palavras-chave: Crescimento. Antioxidantes. Micronutrientes. Fotossíntese. Metabolismo. Selênio. Efeito do ferro.

ABSTRACT

LAPAZ, Allan de Marcos, D.Sc., Universidade Federal de Viçosa, February, 2024. **Selenium as a mitigation of iron deficiency in soybeans**. Advisor: Cleberson Ribeiro. Co-advisers: Maximiller Dal-Bianco Lamas Costa.

Although iron (Fe) is abundant in most agricultural soils, its bioavailability to plants is limited. The Fe deficiency can cause significant changes in plant metabolites, impacting the plant's life cycle. In this context, selenium (Se) has been shown promising effects against Fe deficiency. However, little is known about the role of selenium (Se) in modulating the nutritional status and the non-enzymatic and enzymatic antioxidant defense system in Fe-deficient soybean. In the first experiment, we evaluated the possible beneficial effect of Se applied in the nutrient solution on photosynthetic pigments, nutritional status, reactive oxygen species accumulation, ascorbate and glutathione metabolites, activity of enzymes involved in the synthesis pathway of these metabolites, and antioxidant defense enzymes, including expression of superoxide dismutase (SOD) isoforms, after exposure to absence, deficiency, and sufficiency of Fe in combination with absence and presence of Se. The higher remobilization of Fe associated with maintenance of foliar N concentration resulted in mitigation of leaf chlorosis and decreased loss of photosynthetic pigments in the absence of Fe with Se. Additionally, under this cultivation condition, the main positive effect of Se was shown to be associated with the modulation of the glutathione cycle. The Se supply also reduced the need to replace SOD-Fe with SOD-Cu due to the positive modulation in the crosstalk between Fe and Cu, as well as attenuated the nutritional imbalance of Zn and Mn, mainly in the absence of Fe. These adjustments prevented lipid peroxidation in plants treated with Se. In the second experiment, we evaluated the effects of Se on dry mass, Fe concentration in the roots and shoots, as well as to assess the photosynthetic performance and primary metabolism in soybean plants subjected to Fe deficiency. In the absence of Fe, plants treated with Se exhibited positive modulation in net CO_2 assimilation rate, improving carboxylation efficiency and photochemical traits compared to plants without Se. The synergistic absence of Se and Fe compromised shoot and root dry mass and protein concentration. Therefore, these findings highlight the potential of Se as a valuable intervention to mitigate Fe deficiency in soybean crops.

Keywords: Growth. Antioxidants. Micronutrients. Photosynthesis. Metabolism. Selenium. Iron effect.

LIST OF ILLUSTRATIONS ARTICLE I

LIST OF ILLUSTRATIONS ARTICLE II

LIST OF TABLES ARTICLE I

Sumário

1. Introdução geral

O ferro (Fe) desempenha um papel fundamental no crescimento e desenvolvimento das plantas, sendo essencial para uma variedade de processos fisiológicos (Krohling et al., 2016). Como cofator de várias enzimas, o Fe participa de reações de oxidação-redução, transporte de elétrons e catálise (Hantzis et al., 2018; Kaya et al., 2020), desempenhando um papel crítico na fotossíntese, metabolismo de compostos orgânicos e sistema de defesa antioxidante (Zhang et al., 2019; He et al., 2023).

No entanto, a disponibilidade de Fe para as plantas pode ser limitada em solos agrícolas, mesmo em regiões com abundância de Fe. Isso ocorre devido à baixa solubilidade dos óxidos/hidróxidos de Fe, especialmente em solos com pH neutro a alcalino (Colombo et al., 2018). Como resultado, as plantas frequentemente apresentam sintomas de deficiência de Fe, sendo característico a clorose internerval e a redução do crescimento e desenvolvimento (Kaya et al., 2019).

Além de afetar a biomassa da planta, a deficiência de Fe também prejufica o metabolismo celular. Em particular, a deficiência de Fe perturba as etapas fotoquímicas e bioquímicas da fotossíntese, consequentemente pode desencadear a produção exarcebada de espécies reativas de oxigênio (EROs), resultando em danos oxidativos às células (Wang et al., 2017; He et al., 2023). O Fe também atua como cofator de enzimas antioxidantes, como a superóxido dismutase (SOD), catalase (CAT), peroxidase total (POX) e ascorbato peroxidase (APX), que desempenham um papel crucial na proteção das plantas contra danos oxidativos decorrentes da superprodução dessas moléculas reativas (Zhao et al., 2018; Santos et al., 2019). Assim, a deficiência de Fe compromete o sistema antioxidante enzimático, agravando o desequilíbrio redox celular e afetando negativamente o metabolismo celular das plantas.

Na busca de alternativas para superar a deficiência de Fe e melhorar as respostas fisiológicas das plantas, o selênio (Se) tem despertado interesse entre os fisiologistas (Hajiboland et al. 2020). Embora o Se não seja um nutriente essencial para as plantas, estudos anteriores demonstraram o seu potencial em aumentar a concentração de pigmentos fotossintéticos (Cunha et al., 2022), melhorar as taxas fotossintéticas (Yin et al., 2019), aprimorar o sistema de defesa antioxidante (Elkelish et al., 2019; Djanaguiraman et al., 2005; Yildiztugay et al., 2017; Cunha et al., 2022) e modular o metabolismo do nitrogênio (N) e dos carboidratos (Cunha et al., 2022; Cunha et al., 2023).

Além disso, o Se pode interagir com o metabolismo do enxofre (S), outro elemento essencial para as plantas. Ambos elementos compartilham vias metabólicas comuns e influenciam a absorção e a assimilação um do outro (Ramos et al., 2011; Boldrin et al., 2016). Estudos anteriores relataram que o fornecimento de Se em plantas não acumuladoras desse elemento induz a absorção de S (Ramos et al., 2011; Boldrin et al., 2016; Astolfi et al., 2021). Esse efeito pode ser atribuído à reação do Se com glutationa reduzida (GSH, principal reservatório de S não reduzido a proteína), resultando na

formação de cisteína e metionina contendo Se, e subsequentemente na síntese de selenoproteínas (Feng et al., 2013).

2. Obejetivo Geral

O objetivo geral deste estudo foi investigar o efeito benéfico da suplementação com Se em plantas de soja expostas à deficiência de Fe. Especificamente, este estudo teve como objetivo avaliar o impacto do Se em vários aspectos, incluindo os efeitos do Se sobre a massa seca da parte aérea e das raizes, pigmentos fotossintéticos, características fotossintéticas, metabolismo primário, acúmulo de ROS, peroxidação lipídica e modulação dos metabólitos ascorbato e glutationa, incluindo a atividade de enzimas envolvidas na via de síntese desses metabólitos, sistemas de defesa antioxidante e expressão de isoformas da superóxido dismutase.

References

Astolfi, S., Celletti, S., Vigani, G., Mimmo, T., Cesco, S., 2021. Interaction between sulfur and iron in plants. Front. Plant Sci., 12, 670308. https://doi.org/10.3389/fpls.2021.670308

Boldrin, P.F., de Figueiredo, M.A., Yang, Y., Luo, H., Giri, S., Hart, J.J., Faquin, V., Guilherme, L.R.G., Thannhauser, T.W., Li, L. (2016). Selenium promotes sulfur accumulation and plant growth in wheat (*Triticum aestivum*). Physiol. Plant., 158(1), 80–91. https://doi.org/10.1111/ppl.12465

Colombo, C., Iorio, E.D., Liu, Q., Jiang, Z., Barrón, V. (2018). Iron oxide nanoparticles in soils: environmental and agronomic importance. J. Nanosci. Nanotechnol., 18(1), 761–761. https://doi.org/10.1166/jnn.2018.15294

Cunha, M.L.O., de Oliveira, L.C.A., Mendes, N.A.C., Silva, V.M., Vicente, E.F., dos Reis, A.R. (2023). Selenium Increases Photosynthetic Pigments, Flavonoid Biosynthesis, Nodulation, and Growth of Soybean Plants (*Glycine max* L.). Journal of Soil Science and Plant Nutrition, 1-11. https://doi.org/10.1007/s42729-023-01131-8

Cunha, M.L.O., de Oliveira, L.C.A., Silva, V.M., Montanha, G.S., dos Reis, A.R. (2022). Selenium increases photosynthetic capacity, daidzein biosynthesis, nodulation and yield of peanuts plants (*Arachis hypogaea* L.). Plant Physiology and Biochemistry, 190, 231-239. https://doi.org/10.1016/j.plaphy.2022.08.006

Djanaguiraman, M., Devi, D.D., Shanker, A.K., Sheeba, J.A., Bangarusamy, U. (2005). Selenium–an antioxidative protectant in soybean during senescence. Plant Soil, 272(1), 77–86. https://doi.org/10.1007/s11104-004-4039-1

Elkelish, A.A., Soliman, M.H., Alhaithloul, H.A., El-Esawi, M.A. (2019). Selenium protects wheat seedlings against salt stress-mediated oxidative damage by up-regulating antioxidants and

osmolytes metabolism. Plant Physiol. Biochem., 137, 144–153. https://doi.org/10.1016/j.plaphy.2019.02.004

Feng, R., Wei, C., Tu, S. (2013). The roles of selenium in protecting plants against abiotic stresses. Environ. Exp. Bot., 87, 58–68. https://doi.org/10.1016/j.envexpbot.2012.09.002

Hajiboland, R., Sadeghzadeh, N., Bosnic, D., Bosnic, P., Tolrà, R., Poschenrieder, C., Nikolic, M. (2020). Selenium activates components of iron acquisition machinery in oilseed rape roots. Plant and Soil, 452, 569-586. https://doi.org/10.1007/s11104-020-04599-w

Hantzis, L.J., Kroh, G.E., Jahn, C.E., Cantrell, M., Peers, G., Pilon, M., Ravet, K. (2018). A program for iron economy during deficiency targets specific Fe proteins. Plant Physiology, 176(1), 596-610. https://doi.org/10.1104/pp.17.01497

He, X.L., Zhang, W. Q., Zhang, N.N., Wen, S.M., Chen, J. (2023). Hydrogen sulfide and nitric oxide regulate the adaptation to iron deficiency through affecting Fe homeostasis and thiol redox modification in *Glycine max* seedlings. Plant Physiology and Biochemistry, 194, 1-14. https://doi.org/10.1016/j.plaphy.2022.11.003

Kaya, C., Ashraf, M. (2019). The mechanism of hydrogen sulfide mitigation of iron deficiency-induced chlorosis in strawberry (*Fragaria* × *ananassa*) plants. Protoplasma 256, 371–382. https://doi.org/10.1007/s00709-018-1298-x

Kaya, C., Ashraf, M., Alyemeni, M.N., Ahmad, P., 2020. Nitrate reductase rather than nitric oxide synthase activity is involved in 24-epibrassinolide-induced nitric oxide synthesis to improve tolerance to iron deficiency in strawberry (*Fragaria* × *annassa*) by up-regulating the ascorbate-glutathione cycle. Plant Physiol. Biochem., 151, 486–499. https://doi.org/10.1016/j.plaphy.2020.04.002

Krohling, C.A., Eutrópio, F.J., Bertolazi, A.A., Dobbss, L B., Campostrini, E., Dias, T., Ramos, A.C. (2016). Ecophysiology of iron homeostasis in plants. Soil Science and Plant Nutrition, 62, 39–47. https://doi.org/10.1080/00380768.2015.1123116

Ramos, S.J., Rutzke, M.A., Hayes, R.J., Faquin, V., Guilherme, L.R.G., Li, L. (2011). Selenium accumulation in lettuce germplasm. Planta 233, 649–660. https://doi.org/10.1007/s00425-010-1323-6

Santos, C.S., Ozgur, R., Uzilday, B., Turkan, I., Roriz, M., Rangel, A.O.S.S, Carvalho, S.M.P., Vasconcelos, M.W. (2019). Understanding the role of the antioxidant system and the tetrapyrrole cycle in iron deficiency chlorosis. Plants, 8(9), 348. https://doi.org/10.3390/plants8090348

Wang, Y., Xu, C., Li, K., Cai, X., Wu, M., Chen, G. (2017). Fe deficiency induced changes in rice (*Oryza sativa* L.) thylakoids. Environmental Science and Pollution Research, 24, 1380-1388. https://doi.org/10.1007/s11356-016-7900-x

Yildiztugay, E., Ozfidan-Konakci, C., Kucukoduk, M., Tekis, S.A. (2017). The impact of selenium application on enzymatic and non-enzymatic antioxidant systems in *Zea mays* roots treated with combined osmotic and heat stress. Archives of Agronomy and Soil Science, 63(2), 261–275. https://doi.org/10.1080/03650340.2016.1201810

Zhang, X.Y., Jia, X.M., Zhang, R., Zhu, Z. L., Liu, B., Gao, L. Y., Wang, Y.X. (2019). Metabolic analysis in *Malus halliana* leaves in response to iron deficiency. Scientia Horticulturae, 258, 108792. https://doi.org/10.1016/j.scienta.2019.108792

Zhao, J., Zhang, W., Qiu, Q., Meng, F., Zhang, M., Rao, D., Wang, Z., Yan, X. (2018). Physiological regulation associated with differential tolerance to iron deficiency in soybean. Crop Sci., 58 (3), 1349–1359. https://doi.org/10.2135/cropsci2017.03.0154

Article I

Environmental and Experimental Botany 211 (2023) 105356

Contents lists available at ScienceDirect

Environmental and Experimental Botany

journal homepage: www.elsevier.com/locate/envexpbot

Promising role of selenium in mitigating the negative effects of iron deficiency in soybean leaves

Allan de Marcos Lapaz [a,1], Camila Hatsu Pereira Yoshida [b,2], Juliana Guimarães Vieira [a], Jéssica Nayara Basílio Silva [c], Maximiller Dal-Bianco [c,3], Cleberson Ribeiro [d,*,4]

[a] Departamento de Biologia Vegetal, Universidade Federal de Viçosa, 36570-900 Viçosa, Minas Gerais, Brazil
[b] Departamento de Agronomia, Universidade do Oeste Paulista, 19067-175 Presidente Prudente, São Paulo, Brazil
[c] Departamento de Bioquímica e Biologia Molecular, Universidade Federal de Viçosa, 36570-900 Viçosa, Minas Gerais, Brazil
[d] Departamento de Biologia Geral, Universidade Federal de Viçosa, 36570-900 Viçosa, Minas Gerais, Brazil

https://doi.org/10.1016/j.envexpbot.2023.105356

Abstract: Little is known about the role of selenium (Se) in modulating the nutritional status and the non-enzymatic and enzymatic antioxidant defense system in iron(Fe)-deficient soybean. Hence, this work aimed to evaluate the possible beneficial effect of Se applied in the nutrient solution on photosynthetic pigments, nutritional status, reactive oxygen species accumulation, ascorbate and glutathione metabolites, activity of enzymes involved in the synthesis pathway of these metabolites, and antioxidant defense enzymes, including expression of superoxide dismutase (SOD) isoforms, after exposure to absence, deficiency, and sufficiency of Fe in combination with absence and presence of Se. The experimental design was completely randomized with 5 replications, containing 4 plants per pot. In this work, through physiological, biochemical, and molecular analyses, we observed a beneficial effect of Se in soybean plants with Fe suppression, mainly in the absence of Fe. Thus, in the absence of Fe with Se, there was higher remobilization of Fe and maintenance of foliar N concentration, whichresulted in mitigation of leaf chlorosis and decreased loss of photosynthetic pigments. Additionally, under this cultivation condition, the main positive effect of Se was shown to be associated with the modulation of the glutathione cycle, with increases in the reduced glutathione and total glutathione content, reduced glutathione/oxidized glutathione ratio, and in the activity of the γ-glutamylcysteine synthetase, glutathione peroxidase, and glutathione reductase enzymes. The Se supply also reduced the need to replace SOD-Fe with SOD-Cu due to the positive modulation in the crosstalk between Fe and Cu, as well as attenuated the nutritional imbalance of Zn and Mn, mainly in the absence of Fe. These adjustments prevented lipid peroxidation and showed the beneficial role of Se in Fe-depleted plants.

Keywords: Antioxidant defense system. Cationic micronutrients. Ferric state. *Glycine max* L. Reactive oxygen species.

1. Introduction

Iron (Fe) is an essential element for plants (Krohling et al., 2019), since it plays an essential role in many physiological processes, acting as a structural component of several proteins involved in electron transport chain, oxidation–reduction reactions, and catalysis (Hantzis et al., 2018; Kaya et al., 2020a). Although Fe is abundant in mineral soils, much of it is not readily available for plant uptake due to the poor solubility of its main oxides/hydroxides, especially in neutral to alkaline soils (Colombo et al., 2018).

Interveinal chlorosis, a functional deficiency of Fe in young leaves (Kaya et al., 2020b), is the most common symptom in plants grown in these environments that are poor in available Fe (Kaya et al., 2019). To prevent or treat Fe deficiency, synthetic Fe-chelates are the most used due to their efficiency, however they are highly recalcitrant with a negative impact on the environment (Ylivainio, 2010). Furthermore, the application of inorganic Fe compounds to the soil, as Fe salts and insoluble oxides, are rapidly transform into insoluble compounds, making the supplied Fe unavailable to the plant (Aciksoz et al., 2011).

In Fe-deficient plants, the biosynthesis of cofactors essential for the correct functioning of cellular metabolism is disturbed (Solti et al., 2014), affecting enzymatic reactions and the normal transport of electrons in chloroplasts and mitochondria, which can promote overproduction/accumulation of reactive oxygen species (ROS) (Hantzis et al., 2018; Santos et al., 2019; Dey et al., 2022). Concomitantly, as Fe is a cofactor of different antioxidant enzymes, such as Fe superoxide dismutase (SOD), catalase (CAT), total peroxidase (POX), and ascorbate peroxidase (APX), its deficiency can compromise the enzymatic antioxidant system, favoring further ROS accumulation (Zhao et al., 2018; Santos et al., 2019). In sunflower leaves, Fe deficiency promoted an increase in the Hydrogen peroxide (H_2O_2) content and a decrease in SOD, POX, and APX activity (Ranieri et al., 2001). However, the ROS accumulation in *Arabidopsis thaliana* leaves under Fe deficiency was attenuated with the exogenous supply of reduced ascorbate (AsA) and reduced glutathione (GSH), as well as the ferredoxins levels were restored, emphasizing the importance of AsA and GSH in the preservation of cellular redox homeostasis under Fe deficiency (Ramirez et al., 2013).

AsA and GSH are two important non-enzymatic compounds involved in ROS scavenging (Noctor et al., 2012; Corpas et al., 2015). Hence, the maintenance of the AsA and GSH pool through enzymes involved in the recovery of these metabolites, such as monodehydroascorbate reductase (MDHAR), dehydroascorbate reductase (DHAR) and glutathione reductase (GR), is important for in the ROS scavenging by direct or indirect pathways (Foyer and Noctor, 2011). Thus, AsA and GSH can be used as a substrate for APX and glutathione peroxidase (GPX) enzymes, respectively, catalyze the H_2O_2 decomposition (Foyer and Noctor, 2011). In this context, although selenium (Se) is not an

essential nutrient for plants, it may modulate the antioxidant defense system (Gupta and Gupta, 2017). For example, the activity of the following enzymes was increased under different stressors with Se supply: SOD, CAT, APX, and GR in wheat exposed to salt stress (Elkelish et al., 2019), SOD and GPX in senescing soybean (Djanaguiraman et al., 2005), and SOD, APX, MDHAR, DHAR, GR, and GPX in corn subjected to combined drought and heat stress (Yildiztugay et al., 2017). In this way, the Se supply could be an alternative to mitigate the deleterious effects of Fe deficiency.

However, little is known about the role of Se in modulating of the non-enzymatic (AsA–GSH cycle metabolites) and enzymatic antioxidant defense system and the nutritional status in Fe-deficient plants, especially in relation to sulfur (S), since S and Se share common metabolic pathways (Deng et al., 2021). Previous works have reported that the supply of Se induces the uptake of S in non-Se accumulating plants (Ramos et al., 2011; Boldrin et al., 2016, Astolfi et al., 2021), which is apparently due to the fact that Se reacts with GSH (major reservoir of non-protein reduced S) to form Se-containing cysteine (SeCys) and methionine (SeMet) and ultimately synthesizes Se-containing proteins (Feng et al., 2013). Thus, it is intriguing to hypothesize that Se supply under Fe deficiency can modulate the antioxidant defense system, as well as increase the S concentration in the plant, providing it with a higher GSH content.

To test this hypothesis, soybean [*Glycine max* (L.) Merrill] plants were used because it is sensitive to Fe (Zocchi et al., 2007; Gonzalo et al., 2013) and sometimes cultivated in regions with poor Fe availability (Caliskan et al., 2008; Waters et al., 2018). Additionally, it is one of the main crops in the world that provide vegetable oil and protein-rich foods (Kumar et al., 2021). Based on this, we evaluated the possible beneficial effect of Se applied in the nutrient solution on photosynthetic pigments, nutritional status, ROS accumulation, AsA and GSH metabolites, activity of enzymes involved in the synthesis pathway of these metabolites, and antioxidant defense enzymes, including expression of SOD isoforms, after exposure to different Fe concentrations, being them: absence (0 μM), deficiency (10 μM), and sufficiency (45 μM).

2. Materials and Methods

2.1. Plant material and experimental conditions

The experiment was conducted at the Universidade Federal de Viçosa (20° 45′ S, 42° 54′ W; 650 m above sea level), Brazil. Soybean seeds of the cultivar 'Raio' were obtained from the Brasmax Company. The seeds were disinfected with 1% NaOCl (v/v) for 3 min and then washed with deionized water. The seeds were placed on Germitest® paper rolls and moistened with 100 μM $CaCl_2$ (pH 7.0). Then, the paper rolls were incubated in a cultivation chamber and conditioned in the dark at 25°C for 3 days. After this period, the paper rolls were exposed to light for another 3 days.

On the seventh day, the seedlings were selected based on greater vigor and homogeneity. Next, seedlings were acclimated in polypropylene pots with 2 L in half-strength Clark's solution (pH 5.5) (Clark, 1975) under continuous aeration for two days. The plants were kept in the cultivation chamber at 25 ± 1°C, 200 μmol photons m^{-2} s^{-1} light intensity, 80% relative humidity, and a light/dark cycle of 16/8 h.

Afterwards, on the ninth day, the plants were divided into 2 groups: absence (0 mM) and presence (10 μM) of sodium selenate (Na_2SeO_4) (Hajiboland et al., 2020), which were grown in total-strength Clark's solution (pH 6.0) (Clark, 1975) for 3 days. Subsequently, the seedlings already at the V1 stage (Fehr et al., 1971) were exposed to 3 different concentrations of Fe [applied as Fe-ethylenediaminetetraacetic acid (EDTA)], namely absence (0 μM), deficiency (10 μM), and sufficiency (45 μM), similar to the concentrations used by Qiu et al., (2017), associated with Se absence and presence for 9 days. The nutrient solution was renewed every 3 days, with the pH adjusted daily to 6.0.

After that period, coinciding with the V3 vegetative stage (Fehr et al., 1971), the first fully expanded trifoliate leaf (counting from the apex) was collected to determine biometric traits and for laboratory analysis (frozen in liquid N_2 and stored −80ºC).

2.2. Experimental design

The experimental design was completely randomized and was composed of 6 treatments: 1) without Se + Fe absence; 2) without Se + Fe insufficiency; 3) without Se + Fe sufficiency (control); 4) with Se + Fe absence; 5) with Se + Fe insufficiency; and 6) with Se + Fe sufficiency. The experiment was carried out with 5 repetitions containing 4 plants in each pot. Each plant constituted an experimental unit.

2.3. Leaf symptomatology and development

The first fully expanded trifoliate leaf of each plant was cut and photographed, and then its leaf area was measured with an area meter (LI-COR, LI-300C, Lincoln, Nebraska, USA). The trifoliate leaf was placed in an oven with air circulation at 65°C for 72 h to determine its dry weight. Specific leaf area was calculated as trifoliate leaf area (cm^2) divided by trifoliate leaf dry mass (mg).

2.4. Analysis of photosynthetic pigments

Trifoliate leaf tissue (0.1 g) was homogenized in 2 mL containing 0.5% $CaCO_3$ (w/v). After centrifugation at 3,000×*g* at 4°C for 10 min, the absorbance of the supernatant was read at the following wavelengths: 663.2, 646.8, and 470 nm (Thermo Scientific Evolution 60S, Waltham,

USA). The photosynthetic pigments content was determined using the formulas proposed by Lichtenthaler and Wellburn (1983).

2.5. Quantification of nutritional status

The first fully expanded trifoliate leaf of each plant was oven dried at 65°C for 72 h and ground in a Wiley-type mill. To determine the N concentration, the micro-Kjeldahl analytical method was used, as described by Aguilar et al. (2021). Furthermore, to determine P, K, Ca, Mg, S, Cu, B, Zn, Mn, Fe, and Se concentrations, the dried material was digested in HNO_3–$HClO_4$ (3:2, v/v) at 200°C. The measurements were carried out in an inductively coupled plasma optical emission spectrophotometer (ICP-OES, Optima 8300 DV, Perkin Elmer, Waltham, USA) calibrated with an ICP multi-element standard solution. Blank reagent samples were also used in digestion for quality control (Sarruge and Haag, 1974).

2.6. In situ histochemical localization of superoxide anion radical ($O_2^{\bullet-}$)

The central leaflet of the first fully expanded trifoliate leaf was cut and immersed in 10 mM sodium (Na)-phosphate buffer (pH 7.8) containing 0.1% NBT (v/v). Then, the immersed central leaflet was illuminated for 1 h for the appearance of dark bluish spots (blue formazan precipitates). Stained central leaflets were bleached in acetic acid–glycerol–ethanol (1:1:3, v/v/v) solution at 100ºC and then stored in glycerol–ethanol (1:4, v/v) solution until photographed (Shi et al., 2010).

2.7. Determining $O_2^{\bullet-}$, H_2O_2, and lipid peroxidation content

To determine the $O_2^{\bullet-}$ content, trifoliate leaf tissue (50 mg) was homogenized in a penicillin vial containing 2.1 mL of 20 mM Na-phosphate buffer (pH 7.8), 20 μM NADH, 0.1 mM Na_2–EDTA, and 25.2 mM epinephrine in 0.1 N HCl (Mohammadi and Karr, 2001). After incubation at 28°C for 5 min, the content of adrenochrome accumulated was measured at 480 nm (Thermo Scientific Evolution 60S, Waltham, USA). Superoxide anion radical content was calculated by its molar extinction coefficient of 4.0×10^3 M^{-1} cm^{-1}.

The H_2O_2 content was measured based on the peroxide-mediated oxidation of Fe^{2+}, followed by the reaction of Fe^{3+} with xylenol orange (Gay and Gebicki, 2000). Trifoliate leaf tissue (0.2 g) was homogenized in 2 mL of 50 mM K-phosphate buffer (pH 6.5) containing 1 mM hydroxylamine, followed by centrifugation at 10,000×*g* at 4°C for 15 min. An aliquot of the supernatant was added to a reaction medium containing 100 mM sorbitol, 250 μM $FeNH_4(SO_4)$ in 25 mM H_2SO_4, and 250 μM xylenol orange. Samples were kept in the dark for 30 min, and absorbance of the Fe^{3+}-xylenol orange complex was measured at 560 nm using a microplate reader (Tecan, Infinite M200 PRO, Männedorf, Switzerland). The H_2O_2 content was calculated based on the authentic H_2O_2 standard curve.

Lipid peroxidation was measured based on the content of thiobarbituric acid-reactive substance (TBARS), according to Heath and Packer (1968). Trifoliate leaf tissue (0.2 g) was homogenized in 2 mL of 1% TCA (w/v). After centrifugation at 12,000×*g* at 4°C for 15 min, an aliquot of the supernatant was added to a reaction medium containing 0.5% TBA (w/v) and 20% TCA (w/v), followed by incubation at 95°C for 30 min. After centrifugation (10,000×*g* at 4°C for 10 min), the absorbance of the supernatant was read at two wavelengths (535 and 600 nm) using a microplate reader. The MDA-TBA content complex was estimated using a molar extinction coefficient of 155 × 10^3 M^{-1} cm^{-1}.

2.8. Determining AsA and DHA content

Trifoliate leaf tissue (0.3 g) was homogenized in 2 mL of 6% TCA (w/v) and centrifuged at 12,000×*g* at 4ºC for 12 min. To determine the total ascorbate (tAsA) content, a fraction of the supernatant was incubated at 42ºC for 15 min containing Na-phosphate buffer (pH 7.4) and 10 mM DTT, and then excess DTT was removed by adding 0.5% NEM (w/v). Next, an aliquot was added to a reaction medium containing 2.5% TCA (w/v), 8.4% H_3PO_4 (v/v), 0.8% 2,2'-dipyridyl (w/v) dissolved in 70% ethanol (v/v), and 0.3% $FeCl_3$ (w/v), followed by incubation at 42ºC for 40 min (Kampfenkel et al., 1995). The production of the Fe^{2+} complexes with 2,2'-dipyridyl were measured at 525 nm using a microplate reader. For the determination of AsA content, the step in which DTT and NEM were added was omitted. The tAsA and AsA content were determined based on the calibration curve using AsA standard. Dehydroascorbate (DHA) content was estimated from the difference between the contents of tAsA and AsA.

2.9. Determining GSH and GSSG content

Trifoliate leaf tissue (0.3 g) was homogenized in 2 mL of 0.1 N HCl containing 1 mM EDTA, followed by centrifugation at 12,000×*g* at 4ºC for 10 min. The total glutathione (tGSH) content was measured from the supernatant, whereas the oxidized glutathione (GSSG) content was measured after GSH derivatization by adding the supernatant to 10% 2-VP (v/v) at 30°C for 60 min, then the 2-VP was neutralized with the addition of 17% triethanolamine (v/v). Next, an aliquot of both samples was added to a reaction medium containing 25 mM Na-phosphate buffer (pH 7.5), 0.5 mM DTNB, 0.24 mM NADPH, and 1 U mL^{-1} GR (Rahman et al., 2006). TNB production was monitored at 412 nm using a microplate reader. The rate of change in absorbance was compared with that of GSH standard. GSH content was estimated from the difference between the contents of tGSH and GSSG.

2.10. RNA extraction, cDNA synthesis, and gene expression by qRT–PCR

The RNA was extracted from trifoliate leaf tissue (80 mg) using the Trizol Reagent (Invitrogen) following the manufacturer's recommendation. Next, the RNA was quantified by

spectrophotometer (Nanodrop 2000, Thermo Fisher Scientific). The amount of 2 μg of RNA was treated with DNase I Amplification Grade (Invitrogen) to remove potential contamination with genomic DNA through the following reaction: 2 μg of RNA, 1 μL of 10× DNase I Reaction Buffer, 1 μL of RNaseOUT (Invitrogen), 1 μL of DNase I Amp Grade, and water to 10 μL. After 30 min of incubation at room temperature, 1 μL of 25 mM EDTA was added and heated at 65°C for 10 min. Then, 11 μL of RNA DNase-treated was added for cDNA synthesis using the MMLV Reverse Transcriptase kit (Invitrogen), according to the manufacturer's recommendation.

To investigate the pool of transcripts of SOD subfamilies (Cu/Zn-SOD, Fe-SOD, and Mn-SOD), genes from each SOD subfamily were grouped according to phylogenetic relationship and sequence conservation (Lu et al., 2020). The clusters were arranged as follows: Cu/Zn-SOD1 (*Glyma.03G242900* and *Glyma.19G240400*); Cu/Zn-SOD2 (*Glyma.11G192700*, *Glyma.12G081300*, and *Glyma.12G178800*); Cu/Zn-SOD3 (*Glyma.16G153900*); Mn-SOD1 (*Glyma.04g221300.1* and *Glyma.06g144500.1*); Fe-SOD1 (*Glyma.02g087700.1*, *Glyma.10G117100*, *Glyma.10G193500*, and *Glyma.20G196900*); and Fe-SOD2 (*Glyma.20G050800*) (Supplementary Table 1). The specific primers for each cluster were designed using the Primer3 software (https://primer3.ut.ee/) using the sequence conservation. The CYP (*Glyma.12G024700*) gene was used as internal control (Silva et al., 2022).

Quantitative PCR were performed in a 7500 Real-Time PCR System (Applied Biosystems Foster City, CA) in a 10 μL final volume [1 μL of cDNA diluted 10×, 4 μL of primer at 1.5 μM, and 5 μL of Power SYBR® Green PCR Master Mix (Applied Biosystems, Warrington, UK)]. The amplification reactions were performed under the following conditions: 10 min at 95°C, followed by 40 cycles at 95°C for 15 s, and 1 min at 60–62°C (depending on the primers used). Relative clusters expression levels were calculated by the $2^{-\Delta\Delta Ct}$ method (Livak and Schmittgen, 2001).

2.11. Preparation of crude enzyme extract

The crude L-galactono-y-lactone dehydrogenase (GalLDH) (EC 1.3.2.3) enzyme extract was obtained as described by Li et al. (2010). Trifoliate leaf tissues (0.3 g) were homogenized in 2 mL of 100 mM K-phosphate buffer (pH 7.4) containing 400 mM sucrose, 10% glycerol (v/v), 0.1 mM PMSF dissolved in ethanol, 0.25% mercaptoethanol (v/v), 0.2% Triton X-100 (v/v), and 2% PVPP (w/v). The homogenate was centrifuged at 500×*g* for 10 min at 4°C. After collecting the supernatant, another centrifugation was performed at 20,000×*g* for 20 min at 4°C. Next, the pellet was suspended in 0,3 mL of 100 mM K-phosphate buffer (pH 8.0) containing 10% glycerol (v/v), 5 mM GSH, and 1 mM EDTA. Lastly, the re-suspended solution was centrifuged at 2,000×*g* for 10 min at 4°C.

To extract the other enzymes, trifoliate leaf tissues (0.3 g) were homogenized in the following extraction media: 2 mL of 100 mM K-phosphate buffer (pH 6.8) containing 0.1 mM EDTA, 1 mM

PMSF dissolved in ethanol, and 1% PVPP (w/v) for the enzymes SOD (EC 1.15.1.1), CAT (EC 1.11.1.6), POX (EC 1.11.1.7), and APX (EC 1.11.1.11) (Yoshida et al., 2023)—the extraction buffer for the enzyme APX additionally contained 1 mM AsA; 1.5 mL of 50 mM MES/KOH (pH 6.0) containing 40 mM KCl, 2 mM $CaCl_2$, and 1 mM AsA for the enzymes DHAR (EC 1.8.5.1), MDHAR (EC 1.6.5.4), and GR (EC 1.8.1.7) (Murshed et al., 2008); 2 mL of 100 mM Tris–HCl (pH 8.0) containing 10 mM $MgCl_2$ and 1 mM EDTA for the enzymes γ-glutamylcysteine synthetase (γ-GCS) (EC 6.3.2.2) and glutathione synthetase (GS) (EC 6.3.2.3) (Ramakrishna and Rao 2013); and 2 mL of 100 mM Tris–HCl (pH 7.5) containing 1 mM EDTA and 2 mM DTT for the enzyme GPX (EC 1.11.1.9) (Yoshida et al., 2023). Crude enzyme extracts were collected after centrifugation of the homogenates at 12,000×*g* for 20 min at 4ºC for SOD, CAT, POX, APX, and GPX, at 14,000×*g* for 10 min at 4ºC for MDHAR, DHAR, and GR, and at 10,000×*g* for 15 min at 4ºC for γ-GCS and GS.

2.12. Measurement of enzyme activity

To determine SOD activity, the assay was performed in a reaction chamber under LED light (≅ 1000 lumens) for 3 min and then the photochemical production of blue formazan was measured at 560 nm. The reaction medium contained 50 mM Na-phosphate buffer (pH 7.8), 0.1 mM EDTA, 13 mM methionine, 75 μM NBT, and 2 μM riboflavin (Giannopolitis and Ries, 1977).

CAT activity was estimated through the H_2O_2 decomposition (ε = 36 M^{-1} cm^{-1}) at 240 nm in a reaction medium containing 50 mM K-phosphate buffer (pH 6.8) and 12.5 mM H_2O_2 (Havir and Mchale, 1987). POX activity was determined by measuring purpurogallin production (ε = 2.47 mM^{-1} cm^{-1}) at 420 nm in a reaction medium containing 25 mM K-phosphate buffer (pH 6.8), 20 mM pyrogallol, and 20 mM H_2O_2 (Kar and Mishra, 1976). GalLDH activity was measured by monitoring the rate of cytochrome *c* reduction (ε = 21.3 mM^{-1} cm^{-1}) at 550 nm in a reaction medium containing 50 mM Tris–HCl (pH 8.5), 60 μM cytochorome *c* and 2.5 mM L-galactono-1,4-lactone (Li et al., 2010). APX activity was determined by evaluating the rate of AsA oxidation (ε = 2.8 mM^{-1} cm^{-1}) at 290 nm in a reaction medium containing 50 mM K-phosphate buffer (pH 7.0), 0.1 mM EDTA, 0.5 mM AsA, and 1 mM H_2O_2 (Nakano and Asada, 1981).

DHAR, MDHAR, and GR activity were measured by monitoring the AsA production at 265 nm (ε = 14 mM^{-1} cm^{-1}) and the rate of NADH and NADPH oxidation (ε = 6.22 mM^{-1} cm^{-1}) at 340 nm, respectively. The reaction medium was composed of 50 mM HEPES buffer with pH of 7.0 for DHAR, 7.6 for MDHAR, and 8.0 for GR, containing 0.1 mM EDTA, 2.5 mM GSH, and 0.2 mM DHA in the DHAR assay; 2.5 mM AsA, 0.25 mM NADH, and 2 U mL^{-1} ascorbate oxidase in the MDHAR assay; and 0.5 mM EDTA, 0.25 mM NADPH, and 0.5 mM GSSG in the GR assay (Murshed et al., 2008).

To determine the enzymatic activity of γ-GCS, the crude enzyme extract was added to a reaction medium consisting of 100 mM Tris–HCl buffer (pH 8.2), 2 mM Na_2-EDTA, 10 mM Na-glutamate, 20 mM $MgCl_2$, 10 mM L-aminobutyrate, 0.02% BSA (w/v), and 5 mM Na_2-ATP (Yoshida et al., 2023), whereas the crude enzymatic extract destined for GS was added to a reaction medium consisting of 100 mM Tris–HCl (pH 8.0), 50 mM KCl, 20 mM $MgCl_2$, 1 mM γ-glutamyl-cysteine, 2 mM glycine, 5 mM Na_2-ATP, 5 mM phosphoenolpyruvate, 5 mM DTT, and 10 U mL^{-1} pyruvate kinase (Ramakrishna and Rao, 2013). Next, γ-GCS and GS samples were incubated at 37°C for 30 min. The reaction was stopped by adding 50% TCA (w/v) and then centrifuged at 10,000×*g* for 10 min. The γ-GCS and GS activity were estimated by the inorganic phosphate content in the supernatant determined at 720 nm using the phosphomolybdate method (Lindeman, 1958). GPX activity was measured by monitoring the rate of NADH oxidation (ε = 6.22 mM^{-1} cm^{-1}) in a reaction medium containing 50 mM K-phosphate buffer (pH 7.0), 1 mM Na_2-EDTA, 0.114 M NaCl, 0.2 mM NADPH, 1 mM GSH, 0.25 mM H_2O_2, and 1 U mL^{-1} GR (Nagalashmi and Prasad, 2001).

The total soluble protein in the enzyme extract was determined by the Bradford (1976) method, with BSA as the standard. The activity of all enzymes was determined using a microplate reader.

2.13. Statistical analysis

Normality and homoscedasticity of the data were verified using the Shapiro-Wilk's and Bartlett's tests, respectively, both at 0.05 probability level. Then, the data were subjected to analysis of variance (ANOVA) using the *F* test ($p \leq 0.05$). When significant, the traits were subjected to the Scott-Knott's test ($p < 0.05$). As supplementary analysis, hierarchical clustering, heatmap, and principal component analysis (PCA) were performed using 'pheatmap', 'FactoMineR', 'factoextra', and 'ggplot2' packages. All statistical analysis was performed in the R software (R Development Core Team, 2019).

3. Results

3.1. Leaf symptomatology, leaf development, and photosynthetic pigment content

Nine days after the imposition of treatments, the externalization of leaf chlorosis was observed in the first fully expanded trifoliate leaf only in the absence of Fe, with yellowing more prominent in the plants not treated with Se (Fig. 1a). However, the reductions observed in the absence of Fe in the leaf area, leaf dry weight, and specific leaf area did not differ between the absence and presence of Se (Fig. 1b–d).

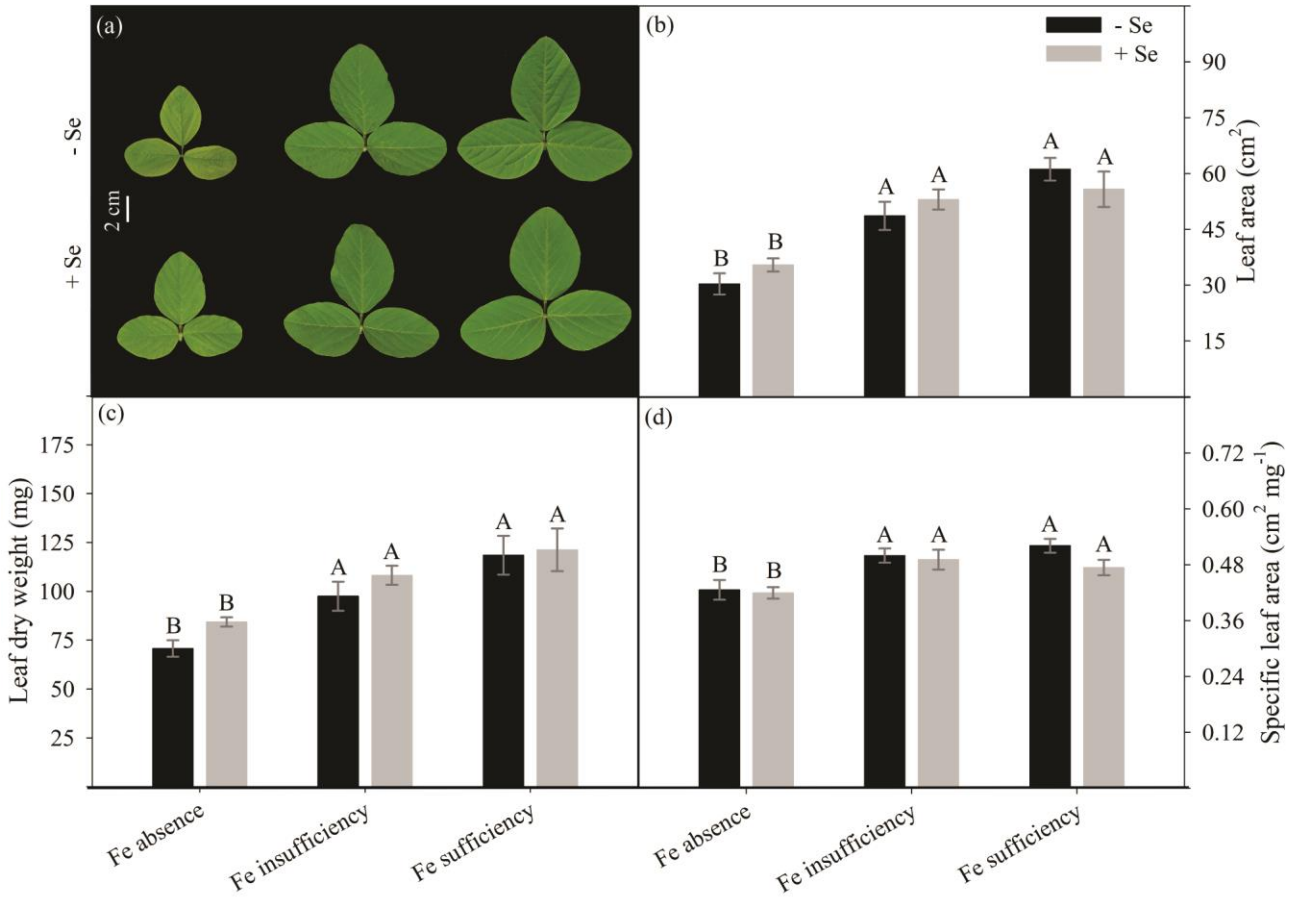

Fig. 1. Leaf symptomatology (adaxial face) (a), leaf area (b), leaf dry weight (c), and specific leaf area (d) of soybean leaves at the V3 phenological stage. Soybean plants were subjected to absence (0 µM), insufficiency (10 µM), and sufficiency of iron (45 µM) for 9 days, associated with the absence (0 µM) or presence of sodium selenate (10 µM), with the beginning of the Se supply 3 days before the imposition of Fe deficiency. Different letters indicate significant differences according to Scott-Knott's test ($p < 0.05$). Bars represent the standard error ($n = 5$ plants).

Chl *a* and CAR content were reduced only in the absence of Fe, mainly in plants not treated with Se, registering decreases of 70 and 61%, respectively, in relation to the control (without Se + Fe sufficiency). Additionally, Chl *b* content was reduced under the absence and insufficiency of Fe but did not differ between the absence and presence of Se. The reduction in TChl content and increase in a/b ratio were more pronounced in the absence of Fe without Se (Table 1).

Table 1. Chlorophyll *a* (Chl *a*), chlorophyll *b* (Chl *b*), total chlorophyll (TChl), and carotenoid (CAR) content and chlorophyll *a*/*b* ratio in soybean leaves at the V3 phenological stage. Soybean plants were subjected to absence (0 μM), insufficiency (10 μM), and sufficiency of iron (45 μM) for 9 days, associated with the absence (0 μM) or presence of sodium selenate (10 μM), with the beginning of the Se supply 3 days before the imposition of Fe deficiency.

Traits	Fe absence		Fe insufficiency		Fe sufficiency	
	-Se	+Se	-Se	+Se	-Se	+Se
	μg g^{-1} FW					
Chl *a*	146.2C ± 14.8	204.9B ± 19.7	453.9A ± 13.2	434.8A ± 21.3	492.4A ± 27.4	486.0A ± 14.8
Chl *b*	23.9C ± 2.5	41.8C ± 4.9	132.4B ± 7.5	124.9B ± 13.4	172.4A ± 9.0	187.4A ± 5.6
TChl	170.2D ± 17.3	246.8C ± 24.5	586.3B ± 20.3	559.7B ± 34.7	664.7A ± 20.8	673.2A ± 32.8
CAR	56.9C ± 4.5	80.1B ± 7.4	139.3A ± 2.9	135.3A ± 7.1	145.6A ± 3.1	143.9A ± 4.1
	No unity					
a/*b* ratio	6.2A ± 0.2	5.0B ± 0.2	3.4C ± 0.1	3.6C ± 0.2	2.9D ± 0.1	2.6D ± 0.1

Different letters indicate significant differences according to Scott-Knott's test ($p < 0.05$). ± means standard error ($n = 5$ plants).

3.2. Nutritional status

Among the macronutrients, there was no variation in the foliar K concentration (Fig. 2c). On the other hand, N concentration was reduced only in the absence of Fe without Se (Fig. 2a). The Ca concentration was similarly reduced under the absence of Fe without and with Se, as well as under the insufficiency of Fe with Se (Fig. 2d). Conversely, the P and Mg concentrations increased in the absence of Fe and did not differ between the absence and presence of Se (Fig. 2b, e). In relation to S concentration, there was a similar increase in its concentration under the absence, insufficiency, and sufficiency of Fe only when associated with the presence of Se (Fig. 2f).

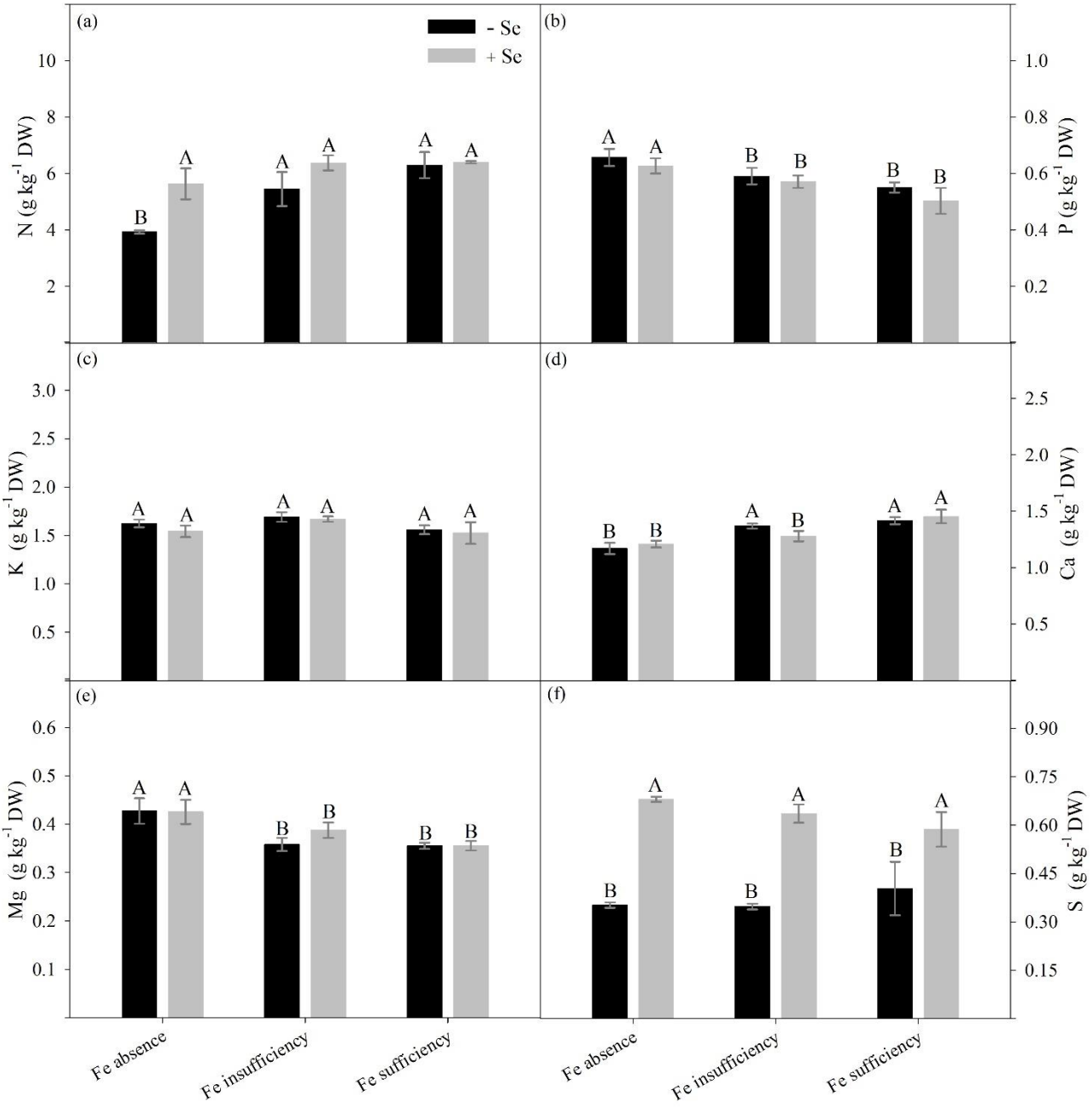

Fig. 2. Nitrogen (a), phosphorus (b), potassium (c), calcium (d), magnesium (e), and sulfur (f), concentrations in soybean leaves at the V3 phenological stage. Soybean plants were subjected to absence (0 µM), insufficiency (10 µM), and sufficiency of iron (45 µM) for 9 days, associated with the absence (0 µM) or presence of sodium selenate (10 µM), with the beginning of the Se supply 3 days before the imposition of Fe deficiency. Different letters indicate significant differences according to Scott-Knott's test ($p < 0.05$). Bars represent the standard error ($n = 5$ plants).

Regarding the micronutrients evaluated, there was no change in the foliar B concentration (Fig. 3b). On the other hand, Cu, Zn, and Mn concentrations increased in the insufficiency and absence of Fe (Fig. 3a, c–d), with the greater increases observed in the absence of Fe without Se, reaching increases of 132, 220, and 298%, respectively, in relation to to control. In contrast, the Fe concentration decreased in the absence of Fe, mainly in plants not treated with Se (Fig. 3e). Regarding

the Se concentration, Se-treated soybean plants showed a similar concentration among the different Fe concentrations tested (Fig. 3f).

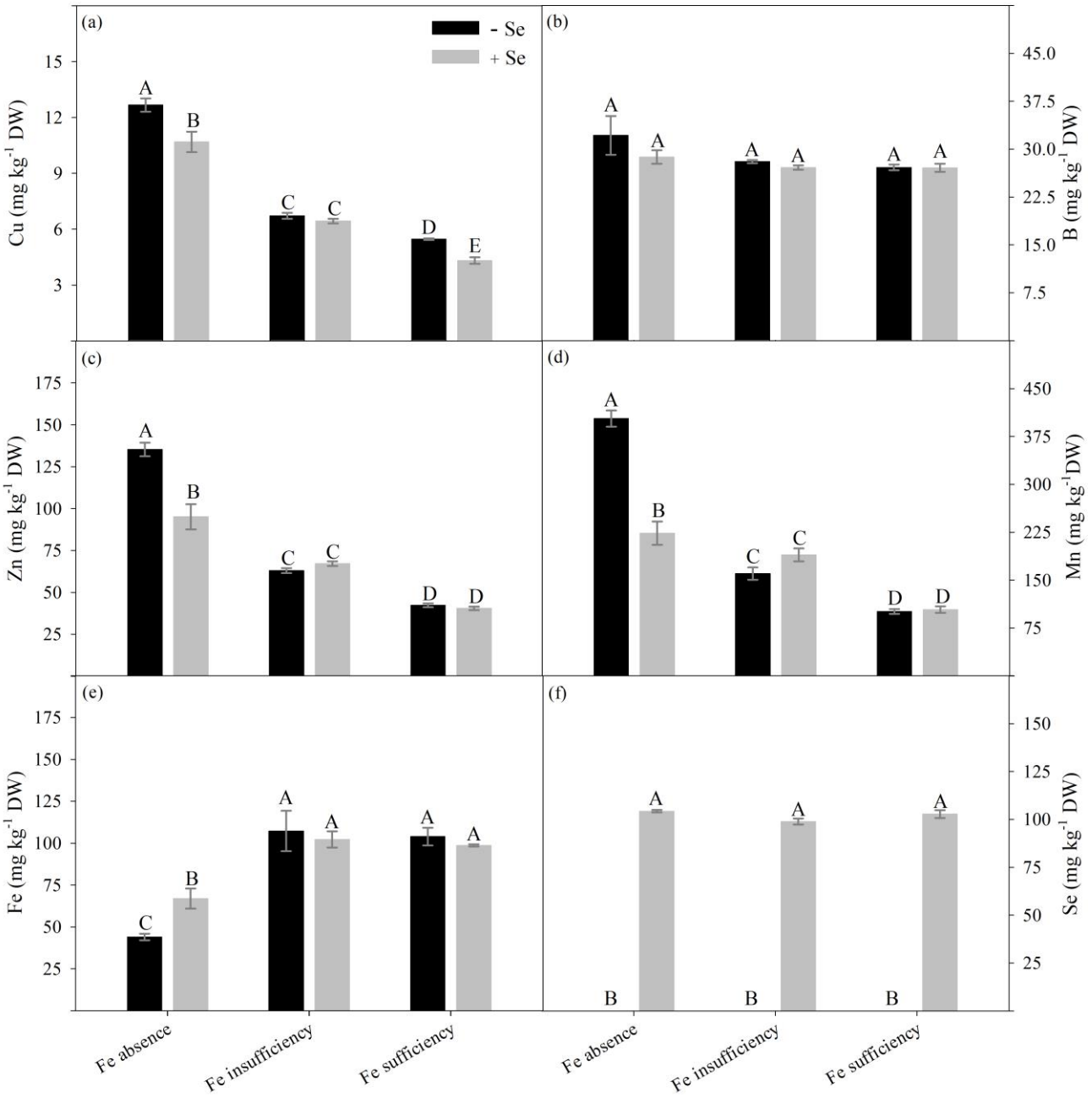

Fig. 3. Copper (a), boron (b), zinc (c), manganese (d), iron (e), and selenium (f) concentrations in soybean leaves at the V3 phenological stage. Soybean plants were subjected to absence (0 µM), insufficiency (10 µM), and sufficiency of iron (45 µM) for 9 days, associated with the absence (0 µM) or presence of sodium selenate (10 µM), with the beginning of the Se supply 3 days before the imposition of Fe deficiency. Different letters indicate significant differences according to Scott-Knott's test ($p < 0.05$). Bars represent the standard error ($n = 5$ plants).

3.3. Oxidative stress

The presence of $O_2^{\bullet-}$ detected on the adaxial epidermis by formazan production was stronger and more diffuse in the absence of Fe, mainly in the plants not treated with Se (Fig. 4a). Furthermore,

on the trifoliate leaf of soybean, the $O_2^{\bullet-}$ content showed a similar response; that is, a higher content in the absence of Fe without Se (Fig. 4b). Regarding the H_2O_2 and MDA content, there was no change in the plants treated with Se, but in the absence of Fe without Se, these traits showed an increase in content (Fig. 4c–d).

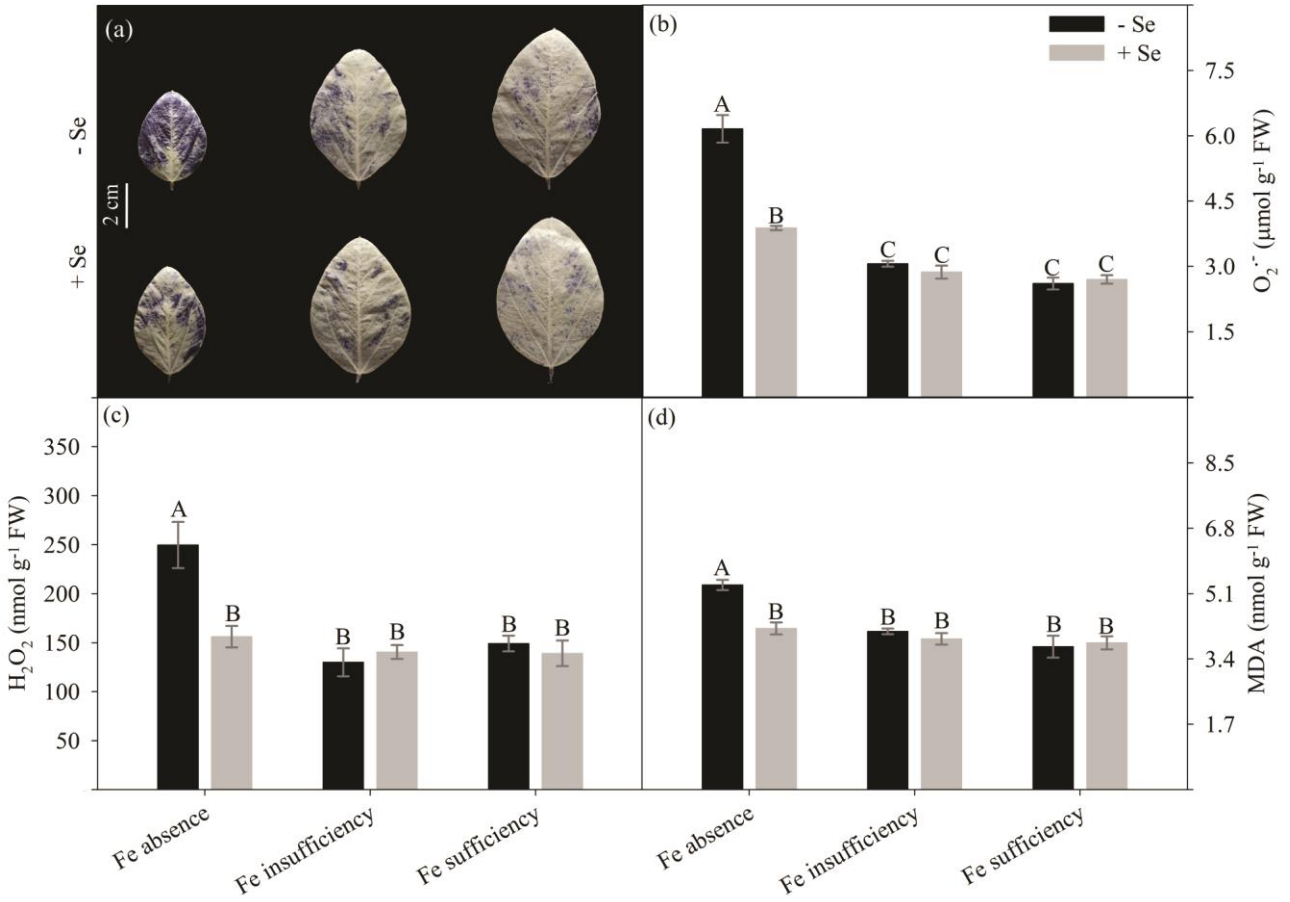

Fig. 4. Histochemical staining of superoxide anion radical by NBT on the leaf adaxial surface (a), and superoxide anion radical (b), hydrogen peroxide (c), and malondialdehyde (d) content in soybean leaves at the V3 phenological stage. Soybean plants were subjected to absence (0 µM), insufficiency (10 µM), and sufficiency of iron (45 µM) for 9 days, associated with the absence (0 µM) or presence of sodium selenate (10 µM), with the beginning of the Se supply 3 days before the imposition of Fe deficiency. Different letters indicate significant differences according to Scott-Knott's test ($p < 0.05$). Bars represent the standard error ($n = 5$ plants).

3.3.1 Antioxidant responses: molecular, enzymatic, and non-enzymatic

Cu/Zn-SOD1 and 2 clusters were upregulated in the insufficiency and absence of Fe. Additionally, in the Cu/Zn-SOD1 cluster, there was a substantial increase (7.5-fould) in the pool of transcribed under the absence of Fe without Se compared to the control. The Cu/Zn-SOD3 cluster expression was not different for any of the studied situations. Mn-SOD1 cluster was upregulated only in the absence of Fe without Se, with a 2.25-fold decrease in relation to the control (Table 2).

The Fe-SOD1 cluster expression was downregulated in the insufficiency and absence of Fe, with the reduction being less prominent in the insufficiency of Fe without Se. In contrast, the Fe-

SOD2 cluster expression upregulated in the insufficiency and absence of Fe (except in the absence of Fe without Se); under these conditions, the largest pool of transcribed was observed in the plants treated with Se (Table 2).

Table 2. Expression of the Cu/Zn-SOD1, 2, and 3; Mn-SOD1; and Fe-SOD1 and 2 clusters in soybean leaves at the V3 phenological stage. Soybean plants were subjected to absence (0 μM), insufficiency (10 μM), and sufficiency of iron (45 μM) for 9 days, associated with the absence (0 μM) or presence of sodium selenate (10 μM), with the beginning of the Se supply 3 days before the imposition of Fe deficiency.

Clusters	Fe absence		Fe insufficiency		Fe sufficiency	
	-Se	+Se	-Se	+Se	-Se	+Se
	Relative expression of the clusters					
Cu/Zn-SOD1	7.69A ± 0.34	3.96B ± 0.16	1.93C ± 0.21	2.37C ± 0.11	1.02D ± 0.11	0.75D ± 0.10
Cu/Zn-SOD2	1.41A ± 0.07	1.73A ± 0.17	2.13A ± 0.19	1.75A ± 0.21	1.01B ± 0.06	0.78B ± 0.14
Cu/Zn-SOD3	0.73A ± 0.05	0.85A ± 0.22	1.33A ± 0.15	1.37A ± 0.17	1.01A ± 0.07	0.79A ± 0.24
Mn-SOD1	2.25A ± 0.19	1.18B ± 0.19	1.56B ± 0.13	1.12B ± 0.20	1.00B ± 0.01	0.73B ± 0.14
Fe-SOD1	0.03C ± 0.003	0.03C ± 0.01	0.61B ± 0.10	0.20C ± 0.02	1.02A ± 0.09	0.62B ± 0.08
Fe-SOD2	1.50C ± 0.11	3.66B ± 0.56	4.03B ± 0.30	5.67A ± 0.53	1.04C ± 0.14	0.67C ± 0.11

Different letters indicate significant differences according to Scott-Knott's test ($p < 0.05$). ± means standard error ($n = 5$ plants).

In the absence and insufficiency of Fe, there was an increase in SOD activity, with the greatest increase observed in the absence of Fe without Se (Fig. 5a). In contrast, CAT and POX activity were reduced in the absence of Fe (without and with Se) and insufficiency of Fe (without Se) (Fig. 5b–c).

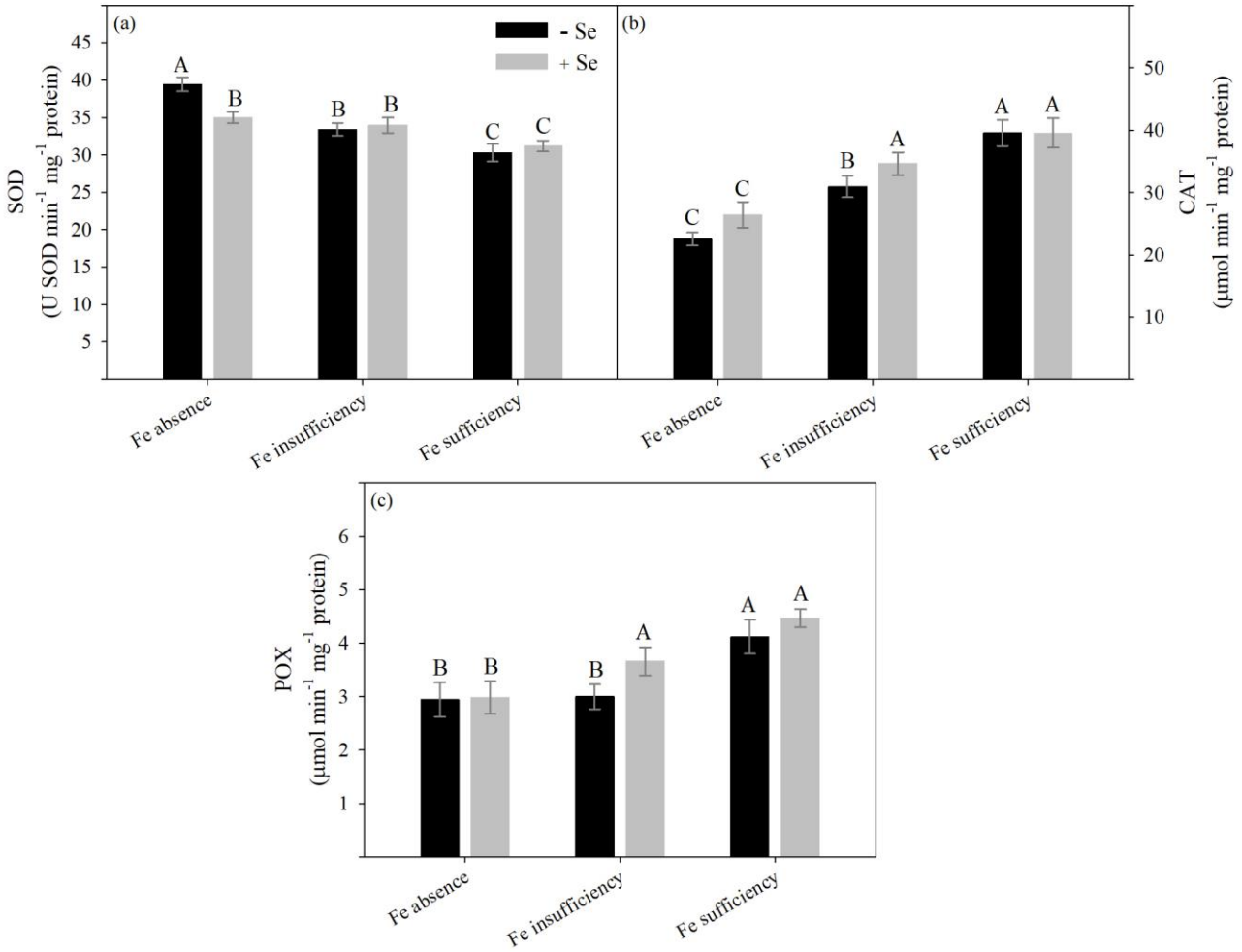

Fig. 5. Superoxide dismutase (a), catalase (b), and total peroxidase (c) activity in soybean leaves at the V3 phenological stage. Soybean plants were subjected to absence (0 µM), insufficiency (10 µM), and sufficiency of iron (45 µM) for 9 days, associated with the absence (0 µM) or presence of sodium selenate (10 µM), with the beginning of the Se supply 3 days before the imposition of Fe deficiency. Different letters indicate significant differences according to Scott-Knott's test ($p < 0.05$). Bars represent the standard error ($n = 5$ plants).

The AsA and tAsA content increased in the absence and insufficiency of Fe, with the highest increases in the plants not treated with Se, except in the absence of Fe for the tAsA content (Fig. 6a, c). Under these conditions, GalLDH activity also increased but did not differ between the absence and presence of Se (Fig. 6e), registering an average increase of 73% in relation to the control. The DHA content was not different for any of the studied situations (Fig. 6b). Furthermore, the AsA/DHA ratio showed the greatest increase in the absence of Fe without Se (Fig. 6d). In the absence of Fe, APX, MDHAR, and DHAR activity were substantially reduced (Fig. 6f–h). Additionally, under the insufficiency of Fe, there were also reductions in APX and DHAR activity (Fig. 6f, h).

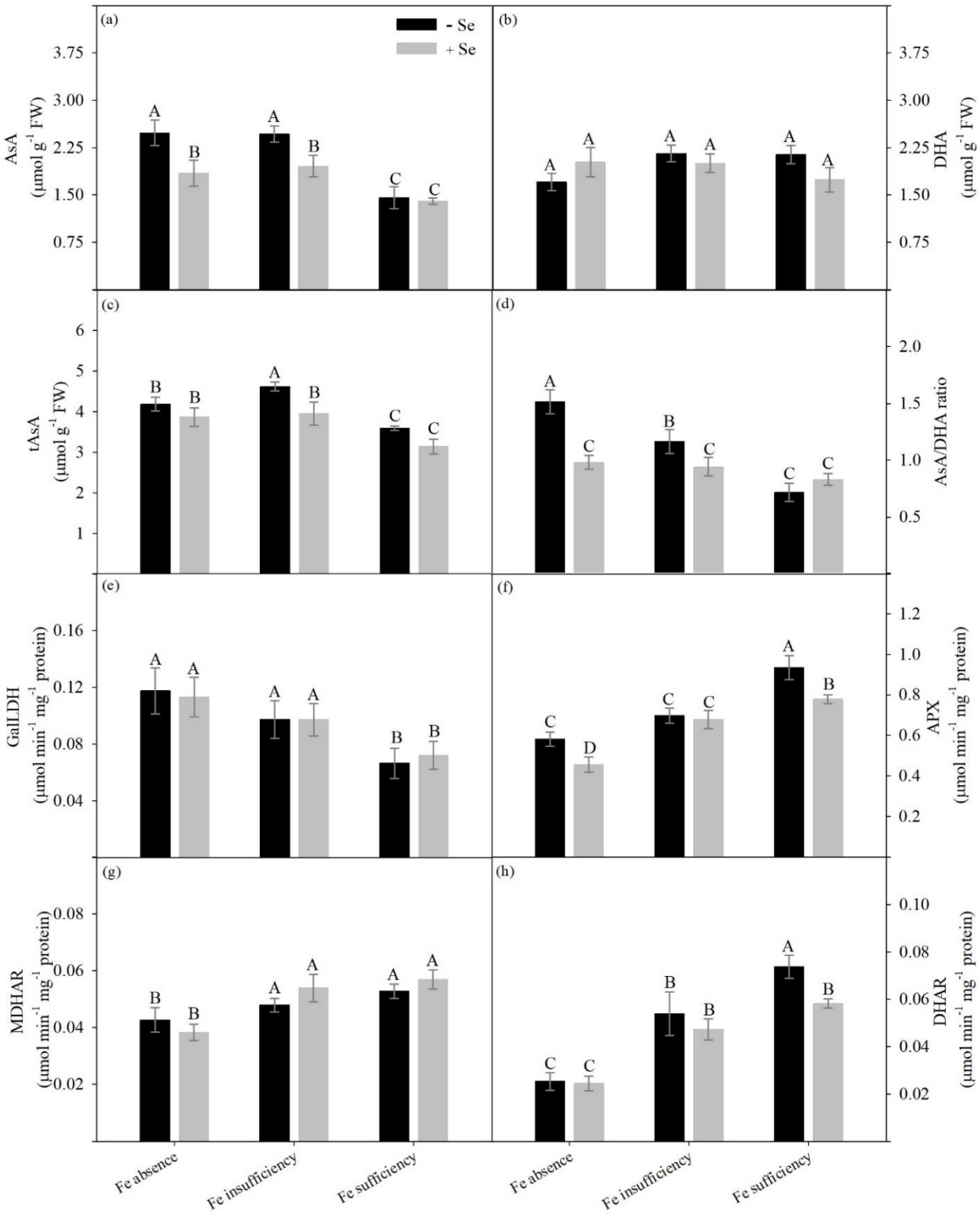

Fig. 6. Ascorbate (a), dehydroascorbate (b), total ascorbate (c), ascorbate/dehydroascorbate ratio (d), L-galactono-γ-lactone dehydrogenase (e), ascorbate peroxidase (f), monodehydroascorbate reductase (g), and dehydroascorbate reductase (h) content/activity in soybean leaves at the V3 phenological stage. Soybean plants were subjected to absence (0 µM), insufficiency (10 µM), and sufficiency of iron (45 µM) for 9 days, associated with the absence (0 µM) or presence of sodium selenate (10 µM), with the beginning of the Se supply 3 days before the imposition of Fe deficiency. Different letters indicate significant differences according to Scott-Knott's test ($p < 0.05$). Bars represent the standard error ($n = 5$ plants).

In the absence and insufficiency of Fe, there was an increase in tGSH content and in GS activity in the presence of Se, with the highest values observed with the complete removal of Fe (Fig. 7c, f). Additionally, in the absence of Fe, GSH content and γ-GCS activity also increased in relation to plants not treated with Se, reaching increases of 32 and 11%, respectively, compared to the control (Fig. 7a, e). Regarding the GSSG content, there was a decrease in the absence and sufficiency of Fe in the plants not treated with Se (Fig. 7b). Furthermore, the GSH/GSSG ratio increased only in the presence of Se, with the increase being more prominent in the absence of Fe (Fig. 7d). Other changes were also observed in the glutathione metabolism under the absence of Fe, as well as increases in GPX (with Se) and GR activity (without and with Se) (Fig. g–h); the increase in GR activity was more pronounced in Se-treated plants (Fig. 7h).

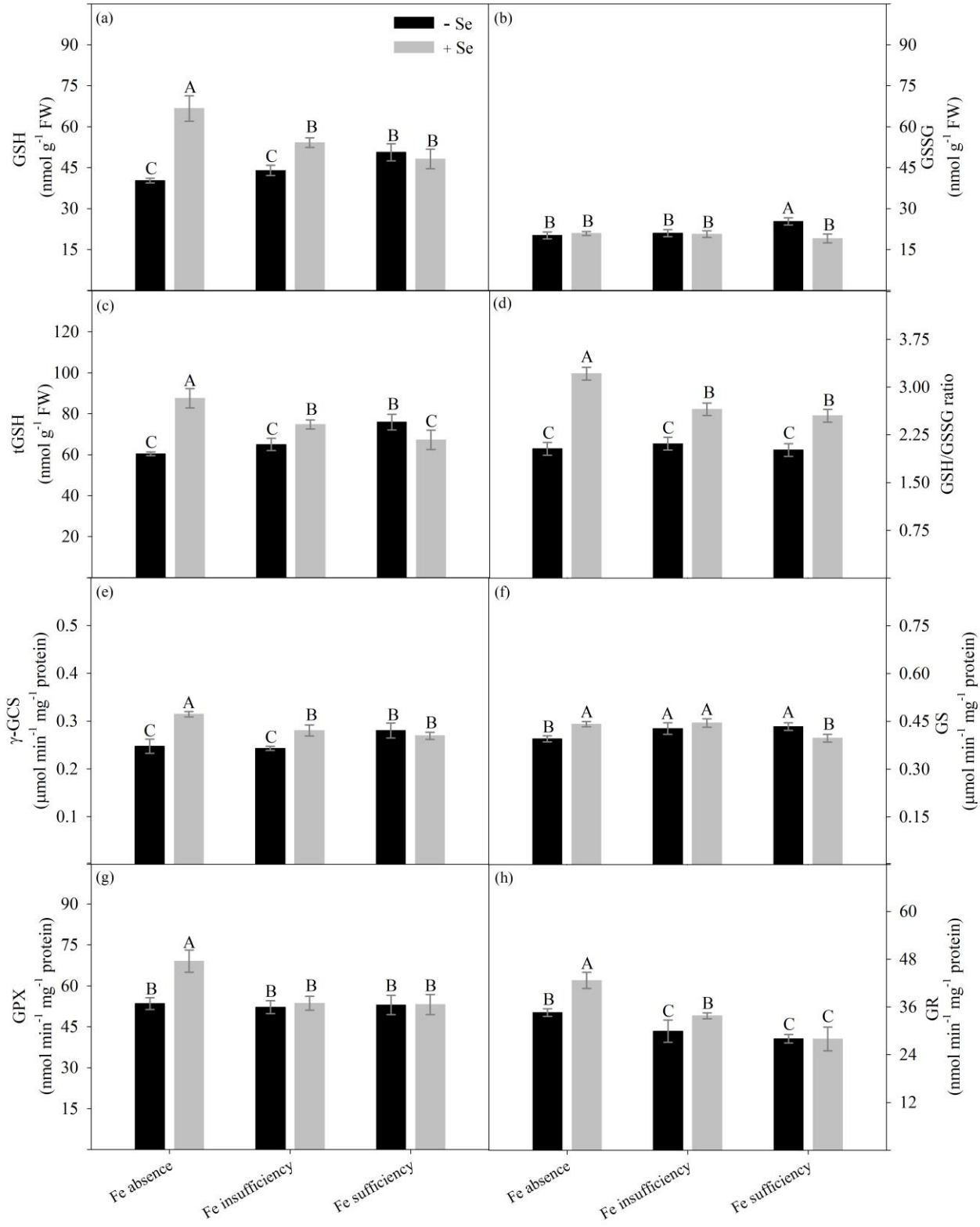

Fig. 7. Reduced glutathione (a), oxidized glutathione (b), total glutathione (c), reduced glutathione/oxidized glutathione ratio (d), γ-glutamylcysteine synthetase (e), glutathione synthetase (f), glutathione peroxidase (g), and glutathione reductase (h) content/activity in soybean leaves at the V3 phenological stage. Soybean plants were subjected to absence (0 µM), insufficiency (10 µM), and sufficiency of iron (45 µM) for 9 days, associated with the absence (0 µM) or presence of sodium selenate (10 µM), with the beginning of the Se supply 3 days before the imposition of Fe deficiency. Different letters indicate significant differences according to Scott-Knott's test ($p < 0.05$). Bars represent the standard error ($n = 5$ plants).

3.4. Hierarchical clustering, heatmap, and PCA

The hierarchical grouping of the analyzed traits was divided into three clusters (1, 2, and 3). In the heatmap, the traits of cluster 1 were negatively modulated in the absence of Fe with or without Se (except GSSG, DHA, and GS) compared to the other treatments. In contrast, the traits of cluster 2 were positively modulated in the absence of Fe with Se in relation to the other treatments, mainly when compared to those without Se. Additionally, in cluster 3, there was an increasing trend for all traits in the absence of Fe without Se, except for K and tAsA, compared to the other treatments (Fig. 8).

From these findings, the greatest modulation of the analyzed traits occurred in the absence of Fe with or without Se, as illustrated by PCA. The treatment of the absence of Fe with Se was strongly associated with cluster 2, whereas the treatment of the absence of Fe without Se was strongly associated with cluster 3. Conversely, the other treatments were moderately (insufficiency of Fe without and with Se) and strongly (sufficiency of Fe without and with Se) associated with cluster 1 (Fig. 8).

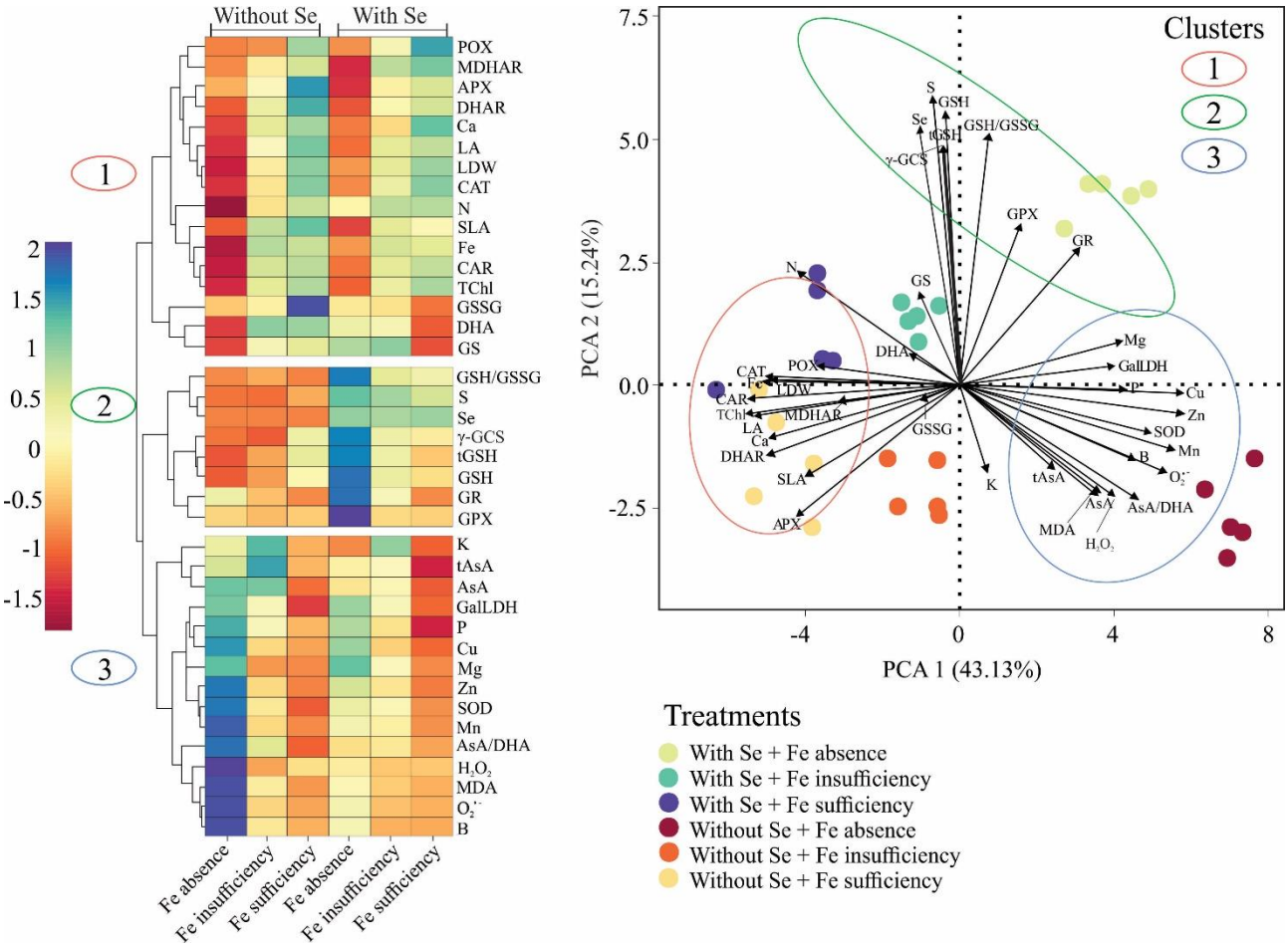

Fig. 8. Hierarchical clustering with heatmap using Euclidean distance and principal component analysis in soybean leaves at the V3 phenological stage. Soybean plants were subjected to absence (0 µM), insufficiency (10 µM), and sufficiency of iron (45 µM) for 9 days, associated with the absence (0 µM) or presence of sodium selenate (10 µM), with the beginning of the Se supply 3 days before the imposition of Fe deficiency. Data were normalized before doing the hierarchical clustering, heatmap, and principal component analysis. Abbreviations: leaf area (LA), leaf dry weight (LDW), specific leaf area (SLA), total chlorophyll (TChl), carotenoid (CAR), nitrogen (N), phosphorus (P), potassium (K), calcium (Ca), magnesium (Mg), sulfur (S), copper (Cu), boron (B), zinc (Zn), manganese (Mn), iron (Fe), selenium (Se), superoxide anion radical ($O_2^{\bullet-}$), hydrogen peroxide (H_2O_2), and malondialdehyde (MDA), superoxide dismutase (SOD), catalase (CAT), total peroxidase (POX), ascorbate (AsA), dehydroascorbate (DHA), total ascorbate (tAsA), ascorbate/dehydroascorbate ratio (AsA/DHA), L-galactono-γ-lactone dehydrogenase (GalLDH), ascorbate peroxidase (APX), monodehydroascorbate reductase (MDHAR), dehydroascorbate reductase (DHAR), reduced glutathione (GSH), oxidized glutathione (GSSG), total glutathione (tGSH), reduced glutathione/oxidized glutathione ratio (GSH/GSSG), γ-glutamylcysteine synthetase (γ-GCS), glutathione synthetase (GS), glutathione peroxidase (GPX), and glutathione reductase (GR).

4. Discussion

In this work, we observed a beneficial effect of Se in soybean plants with Fe suppression. We showed that Se supply was able to attenuate leaf chlorosis, photosynthetic pigment loss, and cationic micronutrient imbalance (Cu, Zn, and Mn), as well as modulation of the non-enzymatic and enzymatic antioxidant defense system, which was essential to prevent lipid peroxidation.

In the absence of Fe, there was a reduction in leaf area, leaf dry weight, and specific leaf area (Fig. 1b–d). This might have been due to impairment in basic metabolic processes, such as photosynthesis (Kaya et al., 2019; Kaya et al., 2020a). On the other hand, in the absence of Fe, leaf chlorosis was attenuated in plants treated with Se (Fig. 1a). As chlorophyll biosynthesis is dependent on Fe–S clusters, specifically the enzymes Mg Proto IX Monomethyl Ester Cyclase and Chlorophyllide A Oxygenase (Kroh and Pilon 2020), the main symptom of Fe deficiency in soybean is interveinal chlorosis of the leaflets, which is most often externalized on newly developed trifoliates (Kaya et al., 2020a) as a consequence of Fe being poorly mobile in the phloem (Malavolta, 1980). Hence, the improvement in Fe-deficiency symptomatology in response to Se supply can be explained by the lower loss of photosynthetic pigments (Table 1), which is due to the increase in the foliar Fe concentration associated with the maintenance of the foliar N concentration (Fig. 2a, 3e, and 8).

In a previous study with oilseed rape, a positive modulation in the Fe uptake mechanism was observed after the supply of Se (Hajiboland et al., 2020). The authors observed that Se up-regulated the expression level of the *FERRIC-REDUCTION OXIDASE* (*FRO1*) gene, as well as increased the activity of the enzyme ferric-chelate reductase (FRO), whose function is to reduce Fe^{3+} (the ferric state) to Fe^{2+} (the ferrous state), increasing the solubility of this element to facilitate its uptake (Lapaz et al., 2022). However, the findings verified by Hajiboland et al. (2020) did not result in a higher foliar Fe concentration in this species. Similar to the present work, in the insufficiency and sufficiency of Fe, Se supply did not provide a higher foliar concentration of Fe in comparison with plants not treated with Se (Fig. 3e). Additionally, the increase foliar concentration of Fe mediated by Se in the absence of Fe was due to greater efficiency in the remobilization of the Fe, since in this treatment, the Fe had been removed from the nutrient solution (Fig. 3e–f).

Besides leaf chlorosis, nutritional imbalance is another common response in Fe-deficient plants (Tomasi et al., 2014, Xie et al., 2019, Rai et al., 2021). In the present study, the imposition of absence of Fe was more harmful for nutritional status than insufficiency of Fe for nutrient concentrations (Fig. 8), except for K and B concentrations, which were not altered in any of the treatments (Fig. 2–3). Under Fe deficiency, it has been reported that P acquisition in both root and shoot is increased (Xie et al., 2019), corroborating with our results (Fig. 2b) and with those of Zheng et al. (2009) in rice. Additionally, in our results, a decrease in Ca concentration was observed in the absence of Fe (Fig. 2d). This phenomenon was also found in Fe-starved plants, such as cucumber (Tomasi et al., 2014), *Eucalyptus* (Lima et al., 2018), and strawberry (Kaya et al., 2019). However, regarding Mg concentration, Lima et al. (2018) found a decrease in the concentration of this element, contrasting with our results (Fig. 2e). Kaya et al. (2019) suggested that the decrease in chlorophyll content in Fe-deficient plants could be associated with a decrease in Mg concentration. However, in

our study, the increase in this element did not show a positive correlation with the chlorophyll content (Fig. 8).

Some of the families of metal transporters involved in intracellular uptake and transport can support multiple metal inputs, such as IRT1, IRT2 (Fe, Zn, and Mn), and NRAMPs (Fe and Mn) (Castaings et al., 2016; Rai et al., 2021), resulting in an increased concentration of these cationic micronutrients (Tomasi et al., 2014), as presented herein (Fig. 3a, c–d). In extreme cases of Fe shortage, an Mn overaccumulation can occur (Therby-Vale, 2021). This phenomenon was observed in this work in the treatment with the absence of Fe without Se, whose treatment triggered higher leaf chlorosis (Fig. 1a and 3d). Surprisingly, besides the aforementioned beneficial effects of Se, this element was also able to mitigate the accumulation of these micronutrients in the absence of Fe (Fig. 8), promoting a higher Fe/Zn and Fe/Mn ratio in relation to plants not treated with Se (Supplementary Table 2).

Upregulation of genes involved in Cu uptake (*COPT2*, *FRO4*, and *FRO5*) in response to Fe deficiency has already been reported in *Arabidopsis thaliana* (Cai et al., 2021). Apparently, this response is a way to increase Cu availability to allow Cu/Zn-SOD isoform to replace Fe-SOD isoform under the Fe shortage (Rai et al., 2021), which is supported by our findings (Fig. 3a, e and Table 2). Cu/Zn-SOD and Fe-SOD are mainly located in the chloroplast and cytoplasm, while Mn-SOD is normally restricted to mitochondria and peroxisomes (Corpas et al., 2015; Rai et al., 2021). In our work, after soybean exposure to the absence and insufficiency of Fe, the transcript pool of the Cu/Zn-SOD isoform was increased by the upregulation of the Cu/Zn-SOD1 and 2 clusters (Table 2). However, for the Fe-SOD isoform, interestingly, only the Fe-SOD1 cluster was downregulated, suggesting a hierarchy in the subcellular allocation of Fe that favors the positive expression of the Fe-SOD2 cluster in the absence of Fe (with Se) and insufficiency of Fe (without and with Se) (Table 2). In rosettes of *A. thaliana*, an increase in the expression of Cu/Zn-SOD genes was also observed to the detriment of a decrease in the expression of Fe-SOD genes under Fe deficiency (Waters et al., 2012).

In parallel to this, notably Se modulates crosstalk between Fe and Cu in the absence of Fe, as observed by the increase in foliar concentration of Fe and decrease in foliar concentration of Cu, resulting in a higher Fe/Cu ratio (Fig. 3a, e and Supplementary Table 2). Apparently, this response resulted in a lower expression of the Cu/Zn-SOD1 cluster and a higher expression of the Fe-SOD2 cluster (Table 2). In this way, the set of these responses suggests a lower need to replace Fe-SOD by Cu/Zn-SOD in plants treated with Se in the absence of Fe.

Fe shortage impairs normal electron transport in chloroplasts and mitochondria and reduces the activity of Fe-dependent antioxidant enzymes, leading to ROS overproduction and lipid peroxidation (Ramírez et al., 2013; Hantzis et al., 2018). Additionally, substantial increases in Cu,

Mn, and Zn concentrations can also result in exacerbated ROS generation (Rai et al., 2021; Therby-Vale, 2021). Indeed, ROS overproduction and MDA increase under the Fe shortage have already been recorded in several plant species, such as strawberry (Kaya et al., 2019; Kaya et al., 2020a), alfalfa (Rahman et al., 2021), and blackgram (Dey et al., 2022). SOD controls the $O_2^{\bullet-}$ amount by its dismutation into H_2O_2, while the H_2O_2 decomposition is catalyzed by CAT and/or POX, such as APX and GPX (Corpas et al., 2015). In the absence of Fe, there was higher SOD activity and higher $O_2^{\bullet-}$ content in plants without Se compared to those with Se (Fig. 4a–b, 5a, and 8), suggesting a greater need for $O_2^{\bullet-}$ scavenging by SOD, which is corroborated by the larger transcript pool detected in most SOD clusters (Cu/Zn-SOD1, Cu/Zn-SOD2, and Mn-SOD1) under the absence of Fe without Se (Table 2). Additionally, under this condition, the H_2O_2 and MDA content also increased (Fig. 4c–d and 8). As CAT and APX contain the heme group in their structure, the low availability of Fe can consequently decrease the activity of these hemoprotein enzymes (Kaya et al., 2020a), limiting H_2O_2 detoxification. Hence, the higher $O_2^{\bullet-}$ and H_2O_2 content associated with lower antioxidant system efficiency in the absence of Fe without Se is related to an increase in MDA content (Fig. 4d and Fig. 8).

AsA is an important metabolite involved in the direct and/or indirect elimination of ROS; for example, it is used as a source of reducing power by the APX enzyme and in the regeneration of oxidized organic molecules, such as tocopherols and carotenoids (Corpas et al., 2015; Xiao et al., 2021). Soybean plants increased AsA content in the absence and insufficiency of Fe, however the increase in AsA content was less pronounced in plants treated with Se, consequently the AsA/DHA ratio remained constant in the absence of Se (Fig 6a, d). This increase in AsA pool in response to Fe deficiency is related to the suppression of APX activity (Guo et al., 2017). Additionally, Kaya et al. (2020a) also observed a substantial reduction in APX activity in strawberry leaves, corroborating with the results found herein, which makes this H_2O_2 detoxification pathway less efficient under these conditions studied, especially when supplied with Se (Fig. 8).

Plants can adjust the cellular amount of AsA through its biosynthesis and/or the regeneration (Xiao et al., 2021). As the MDHAR and DHAR enzymes, responsible for recovering AsA, had their activities substantially reduced (Fig 6g–h), whereas GalLDH activity was increased (Fig. 6e), it is suggestive that the modulation in the AsA pool is due to predominantly to the process of AsA biosynthesis (Fig. 8), which is supported by the presence of increment in tAsA content (Fig. 6c). GalLDH participates in the last step of the main AsA biosynthesis pathway (L-galactose pathway), catalyzing the oxidation of L-galactono-1,4-lactone to AsA, without the participation of redox cofactor (Corpas et al., 2015; Zheng et al., 2022). However, in fiber-bearing cotton ovules, genes of this pathway were suppressed in Fe deficiency, whereas the genes of myo-inositol and galacturonic

acid pathways were activated (Guo et al., 2017), which does not rule out the possibility that these pathways may also be acting in soybean leaves, as an additional source of AsA in the Fe shortage.

In parallel to this, there was an increase in the GSH content in soybean plants in Se-treated plants exposed to Fe suppression (Fig 7a). One of the main functions of GSH is to maintain the AsA–GSH cycle functional, other than that, it also performs other functions, such as the storage and long-distance transport of S (Foyer and Noctor, 2011; Shanmugam et al., 2015). Previously, it was found that the exogenous supply of GSH prevents leaf chlorosis and restores the ferredoxin levels under Fe deficiency, giving greater tolerance to this nutritional stress in *Arabidopsis thaliana* plants (Ramirez et al., 2013). In the present work, it is notable that the increase in the GSH pool mediated by Se is due to modulation in the biosynthesis process, more precisely of the γ-GCS, which catalyzes the synthesis of γ-glutamylcysteine from cysteine and glutamate, as well as through the regeneration process, in which GSSG is recycled to GSH by the NADH-dependent GR (Fig. 7a–b, e, h; Foyer and Noctor, 2011). Hence, the plants treated with Se showed higher redox capacity due to the increase in GSH/GSSG ratio (Fig. 7d), favoring H_2O_2 decomposition by GSH-dependent GPX (Fig. 7g and 8; Foyer and Noctor, 2011), which is in congruence with the antioxidant role of Se in modulating oxidative stress by enhancing the enzymatic and non-enzymatic defense system (Djanaguiraman et al., 2005; Hasanuzzaman et al., 2011; Elkelish et al., 2019). Thus, under Fe shortage, the enhancement of this pathway may be more advantageous for plants in the Fe use hierarchy, since GPX does not use Fe as a cofactor, and is widely distributed in different organelles, including chloroplasts and mitochondria. Takeda et al. (1997) observed that without the Se supply, external H_2O_2 in *Chlamydomonas* cells is found to be decomposed by the APX and CAT, on the other hand, with the Se supply, H_2O_2 is mainly scavenged by GPX instead of APX and CAT, evidencing the Se role in the differential modulation of the pathways involved in ROS scavenged.

Furthermore, some steps involved in the process of incorporation of S and Se into amino acids are GSH dependent (Feng et al., 2013), as well as both elements share common metabolic pathways in plants, which is due to the similar chemical and physical properties (Deng et al., 2021). For example, adenosine 5′-phosphosulfate/selenate (APS and APSe, respectively) are reduced by APS reductase to selenite/sulfite (EC 1.8.4.9), using electrons from GSH. Furthermore, selenite and GSH, in an alternative pathway, are converted nonenzymatically to selenodiglutathione (GSSeSG), which is further converted to selenopersulfide (GSSeH) and finally to selenide by GR (Schiavon et al., 2017). Hence, there is evidence that the increase in the GSH pool is related to greater assimilation of S and Se (Fig. 8). In previous studies, synergism between S and Se in non-accumulating species had already been reported (Ramos et al., 2011; Astolfi et al., 2021), which apparently is due to the fact that Se mimics S deficiency by activating expression of the specific sulfate transporter to stimulate S uptake (Boldrin et al., 2016).

5. Conclusion

The higher remobilization of Fe associated with maintenance of foliar N concentration resulted in mitigation of leaf chlorosis and decreased loss of photosynthetic pigments in the absence of Fe with Se. Additionally, under this cultivation condition, the main positive effect of Se was shown to be associated with the modulation of the glutathione cycle, with increases in the GSH and tGSH content, GSH/GSSG ratio, and in the activity of the γ-GCS, GS, GPX, and GR enzymes. The Se supply also reduced the need to replace SOD-Fe with SOD-Cu due to the positive modulation in the crosstalk between Fe and Cu, as well as attenuated the nutritional imbalance of Zn and Mn, mainly in the absence of Fe. These adjustments prevented lipid peroxidation in plants treated with Se. Thus, our findings suggest that Se supply could be a promising strategy for mitigating the negative effects of Fe deficiency on plant growth and development.

References

Aciksoz, S.B., Yazici, A., Ozturk, L., Cakmak, I., 2011. Biofortification of wheat with iron through soil and foliar application of nitrogen and iron fertilizers. Plant and Soil, 349, 215-225. https://doi.org/10.1007/s11104-011-0863-2

Aguilar, J.V., Lapaz, A.M., Sanches, C.V., Yoshida, C.H.P., Camargos, L.S.D., Furlani-Júnior, E., 2021. Application of 2, 4-D hormetic dose associated with the supply of nitrogen and nickel on cotton plants. Journal of Environmental Science and Health, Part B, 56 (9), 852–859. https://doi.org/10.1080/03601234.2021.1966280

Astolfi, S., Celletti, S., Vigani, G., Mimmo, T., Cesco, S., 2021. Interaction between sulfur and iron in plants. Front. Plant Sci., 12, 670308. https://doi.org/10.3389/fpls.2021.670308

Boldrin, P.F., de Figueiredo, M.A., Yang, Y., Luo, H., Giri, S., Hart, J.J., Faquin, V., Guilherme, L.R.G., Thannhauser, T.W., Li, L., 2016. Selenium promotes sulfur accumulation and plant growth in wheat (*Triticum aestivum*). Physiol. Plant., 158 (1), 80–91. https://doi.org/10.1111/ppl.12465

Bradford, M.M., 1976. A rapid and sensitive method for the quantitation of microgram quantities of protein utilizing the principle of protein-dye binding. Anal. Biochem., 72 (1–2), 248–254. https://doi.org/10.1016/0003-2697(76)90527-3

Caliskan, S., Ozkaya, I., Caliskan, M.E., Arslan, M., 2008. The effects of nitrogen and iron fertilization on growth, yield and fertilizer use efficiency of soybean in a Mediterranean-type soil. Field Crops Res., 108 (2), 126–132. https://doi.org/10.1016/j.fcr.2008.04.005

Castaings, L., Caquot, A., Loubet, S., Curie, C., 2016. The high-affinity metal transporters NRAMP1 and IRT1 team up to take up iron under sufficient metal provision. Sci Rep 6 (1), 1–11. https://doi.org/10.1038/srep37222

Clark, R.B., 1975. Characterization of phosphatase of intact maize roots. J. Agric. Food Chem., 23 (3), 458–460. https://doi.org/10.1021/jf60199a002

Colombo, C., Iorio, E.D., Liu, Q., Jiang, Z., Barrón, V., 2018. Iron oxide nanoparticles in soils: environmental and agronomic importance. J. Nanosci. Nanotechnol., 18 (1), 761–761. https://doi.org/10.1166/jnn.2018.15294

Corpas, F.J., Gupta, D.K., Palma, J.M., 2015. Production sites of reactive oxygen species (ROS) in organelles from plant cells. In Reactive oxygen species and oxidative damage in plants under stress (pp. 1–22). Springer, Cham. https://doi.org/10.1007/978-3-319-20421-5_1

Deng, X., Zhao, Z., Lv, C., Zhang, Z., Yuan, L., Liu, X., 2021. Effects of sulfur application on selenium uptake and seed selenium speciation in soybean (*Glycine max* L.) grown in different soil types. Ecotoxicology and Environmental Safety, 209, 111790. https://doi.org/10.1016/j.ecoenv.2020.111790

Dey, S., Chowardhara, B., Regon, P., Kar, S., Saha, B., Panda, S.K., 2022. Iron deficiency in blackgram (*Vigna mungo* L.): redox status and antioxidant activity. Plant Biosystems-An International Journal Dealing with all Aspects of Plant Biology, 156 (2), 411–426. https://doi.org/10.1080/11263504.2020.1866093

Djanaguiraman, M., Devi, D.D., Shanker, A.K., Sheeba, J.A., Bangarusamy, U., 2005. Selenium–an antioxidative protectant in soybean during senescence. Plant Soil, 272 (1), 77–86. https://doi.org/10.1007/s11104-004-4039-1

Elkelish, A.A., Soliman, M.H., Alhaithloul, H.A., El-Esawi, M.A., 2019. Selenium protects wheat seedlings against salt stress-mediated oxidative damage by up-regulating antioxidants and osmolytes metabolism. Plant Physiol. Biochem., 137, 144–153. https://doi.org/10.1016/j.plaphy.2019.02.004

Fehr, W.R., Caviness, C.E., Burmood, D.T., Pennington, J.S., 1971. Stage of development descriptions for soybeans, *Glycine Max* (L.) Merrill. Crop Sci., 11 (6), 929–931. https://doi.org/10.2135/cropsci1971.0011183X001100060051x

Feng, R., Wei, C., Tu, S., 2013. The roles of selenium in protecting plants against abiotic stresses. Environ. Exp. Bot., 87, 58–68. https://doi.org/10.1016/j.envexpbot.2012.09.002

Foyer, C.H., Noctor, G., 2011. Ascorbate and glutathione: the heart of the redox hub. Plant Physiol., 155 (1), 2–18. https://doi.org/10.1104/pp.110.167569

Gay, C., Gebicki, J.M., 2000. A critical evaluation of the effect of sorbitol on the ferric–xylenol orange hydroperoxide assay. Anal. Biochem., 284 (2), 217–220. https://doi.org/10.1006/abio.2000.4696

Giannopolitis, C.N., Ries, S.K., 1977. Superoxide dismutases: I. Occurrence in higher plants. Plant Physiol., 59 (2), 309–314. https://doi.org/10.1104/pp.59.2.309

Gonzalo, M.J., Lucena, J.J., Hernández-Apaolaza, L., 2013. Effect of silicon addition on soybean (*Glycine max*) and cucumber (*Cucumis sativus*) plants grown under iron deficiency. Plant Physiol. Biochem., 70, 455–461. https://doi.org/10.1016/j.plaphy.2013.06.007

Guo, K., Tu, L., Wang, P., Du, X., Ye, S., Luo, M., Zhang, X., 2017. Ascorbate alleviates Fe deficiency-induced stress in cotton (*Gossypium hirsutum*) by modulating ABA levels. Front. Plant Sci., 7, 1997. https://doi.org/10.3389/fpls.2016.01997

Gupta, M., Gupta, S., 2017. An overview of selenium uptake, metabolism, and toxicity in plants. Front. Plant Sci., 7, 2074. https://doi.org/10.3389/fpls.2016.02074

Hajiboland, R., Sadeghzadeh, N., Bosnic, D., Bosnic, P., Tolrà, R., Poschenrieder, C., Nikolic, M., 2020. Selenium activates components of iron acquisition machinery in oilseed rape roots. Plant Soil, 452 (1), 569–586. https://doi.org/10.1007/s11104-020-04599-w

Hantzis, L.J., Kroh, G.E., Jahn, C.E., Cantrell, M., Peers, G., Pilon, M., Ravet, K., 2018. A program for iron economy during deficiency targets specific Fe proteins. Plant Physiol., 176 (1), 596–610. https://doi.org/10.1104/pp.17.01497

Hasanuzzaman, M., Hossain, M.A., Fujita, M. 2011. Selenium-induced up-regulation of the antioxidant defense and methylglyoxal detoxification system reduces salinity-induced damage in rapeseed seedlings. Biol Trace Elem Res., 143, 1704–1721. https://doi.org/10.1007/s12011-011-8958-4

Havir, E.A., McHale, N.A., 1987. Biochemical and developmental characterization of multiple forms of catalase in tobacco leaves. Plant Physiol., 84 (2), 450–455. https://doi.org/10.1104/pp.84.2.450

Heath, R.L., Packer, L., 1968. Photoperoxidation in isolated chloroplasts: I. Kinetics and stoichiometry of fatty acid peroxidation. Arch. Biochem. Biophys., 125 (1), 189–198. https://doi.org/10.1016/0003-9861(68)90654-1

Kampfenkel, K., Vanmontagu, M., Inze, D., 1995. Extraction and determination of ascorbate and dehydroascorbate from plant tissue. Anal. Biochem., 225 (1), 165–167. https://doi.org/10.1006/abio.1995.1127

Kar, M., Mishra, D., 1976. Catalase, peroxidase, and polyphenoloxidase activities during rice leaf senescence. Plant Physiol., 57 (2), 315–319. https://doi.org/10.1104/pp.57.2.315

Kaya, C., Ashraf, M., 2019. The mechanism of hydrogen sulfide mitigation of iron deficiency-induced chlorosis in strawberry (*Fragaria* × *ananassa*) plants. Protoplasma 256, 371–382. https://doi.org/10.1007/s00709-018-1298-x

Kaya, C., Ashraf, M., Alyemeni, M.N., Ahmad, P., 2020a. Nitrate reductase rather than nitric oxide synthase activity is involved in 24-epibrassinolide-induced nitric oxide synthesis to improve tolerance to iron deficiency in strawberry (*Fragaria* × *annassa*) by up-regulating the ascorbate-glutathione cycle. Plant Physiol. Biochem., 151, 486–499. https://doi.org/10.1016/j.plaphy.2020.04.002

Kaya, C., Higgs, D., Ashraf, M., Alyemeni, M.N., Ahmad, P., 2020b. Integrative roles of nitric oxide and hydrogen sulfide in melatonin-induced tolerance of pepper (*Capsicum annuum* L.) plants to iron deficiency and salt stress alone or in combination. Physiologia plantarum, 168, 256-277. https://doi.org/10.1111/ppl.12976

Kroh Gretchen, E., Pilon, M., 2020. Regulation of iron homeostasis and use in chloroplasts. Int. J. Mol. Sci. 21 (9), 3395. https://doi.org/10.3390/ijms21093395

Kumar, V., Vats, S., Kumawat, S., Bisht, A., Bhatt, V., Shivaraj, S. M., Padalkar, G., Goyal, V., Zargar, S., Gupta, S., Kumawat, G., Chandra, S., Chalam, V.C., Ratnaparkhe, M.B., Gill, B.S., Jean, M., Patil, G.B., Vuong, T., Rajcan, I., Deshmukh, R., Belzile, F., Sharma, T.R., Nguyen, H.T., Sonah, H., 2021. Omics advances and integrative approaches for the simultaneous improvement of seed oil and protein content in soybean (*Glycine max* L.). Critical Reviews in Plant Sciences, 40 (5), 398–421. https://doi.org/10.1080/07352689.2021.1954778

Li, M., Ma, F., Guo, C., Liu, J., 2010. Ascorbic acid formation and profiling of genes expressed in its synthesis and recycling in apple leaves of different ages. Plant Physiol. Biochem., 48 (4), 216–224. https://doi.org/10.1016/j.plaphy.2010.01.015

Lichtenthaler, H.K., Wellburn, A.R., 1983. Determinations of total carotenoids and chlorophylls *a* and *b* of leaf extracts in different solvents. Biochem Soc Trans., 11 (5), 591–592 https://doi.org/10.1042/bst0110591

Lima, M.D.R., Barros Junior, U.D.O., Batista, B.L., Lobato, A.K.D.S., 2018. Brassinosteroids mitigate iron deficiency improving nutritional status and photochemical efficiency in *Eucalyptus urophylla* plants. Trees, 32 (6), 1681–1694. https://doi.org/10.1007/s00468-018-1743-7

Lindeman, W., 1958. Observations on the behavior of phosphate compounds in *Chlorella* at the transition from dark to light. In: Proceedings of the II International Conference on the Peaceful Uses of Atomic Energy. New York (USA): Columbia University. p. 8–15

Livak, K.J., Schmittgen, T.D., 2001. Analysis of relative gene expression data using real-time quantitative PCR and the $2^{-\Delta\Delta CT}$ method. Methods, 25 (4), 402–408. https://doi.org/10.1006/meth.2001.1262

Lu, W., Duanmu, H., Qiao, Y., Jin, X., Yu, Y., Yu, L., Chen, C., 2020. Genome-wide identification and characterization of the soybean SOD family during alkaline stress. PeerJ 8, e8457. https://doi.org/10.7717/peerj.8457

Malavolta, E., 1980. Elementos de nutrição mineral de plantas (Vol. 1, pp. 163–166). São Paulo: Agronômica Ceres.

Mohammadi, M., Karr, A.L., 2001. Superoxide anion generation in effective and ineffective soybean root nodules. J. Plant Physiol., 158 (8), 1023–1029. https://doi.org/10.1078/S0176-1617(04)70126-1

Murshed, R., Lopez-Lauri, F., Sallanon, H., 2008. Microplate quantification of enzymes of the plant ascorbate–glutathione cycle. Anal. Biochem., 383 (2), 320–322. https://doi.org/10.1016/j.ab.2008.07.020

Nagalakshmi, N., Prd, M.N.V., 2001. Responses of glutathione cycle enzymes and glutathione metabolism to copper stress in *Scenedesmus bijugatus*. Plant Sci., 160 (2), 291–299. https://doi.org/10.1016/S0168-9452(00)00392-7

Nakano, Y., Asada, K., 1981. Hydrogen peroxide is scavenged by ascorbate-specific peroxidase in spinach chloroplasts. Plant Cell. Physiol., 22 (5), 867–880. https://doi.org/10.1093/oxfordjournals.pcp.a076232

Noctor, G., Mhamdi, A., Chaouch, S., Han, Y.I., Neukermans, J., Marquez-Garcia, B.E., Queval, G., Foyer, C.H., 2012. Glutathione in plants: an integrated overview. Plant, cell & environment, 35 (2), 454–484. https://doi.org/10.1111/j.1365-3040.2011.02400.x

Qiu, W., Dai, J., Wang, N., Guo, X., Zhang, X., Zuo, Y., 2017. Effects of Fe-deficient conditions on Fe uptake and utilization in P-efficient soybean. Plant Physiol. Biochem., 112, 1–8. https://doi.org/10.1016/j.plaphy.2016.12.010

R Core Team. R: A language and environment for statistical computing. R Foundation for Statistical Computing, Vienna, Austria. 2018. Available in: https://www.R-project.org/

Rahman, I., Kode, A., Biswas, S.K., 2006. Assay for quantitative determination of glutathione and glutathione disulfide levels using enzymatic recycling method. Nat. Protoc., 1 (6), 3159–3165. https://doi.org/10.1038/nprot.2006.378

Rahman, M.A., Kabir, A.H., Song, Y., Lee, S.H., Hasanuzzaman, M., Lee, K.W., 2021. Nitric oxide prevents Fe deficiency-induced photosynthetic disturbance, and oxidative stress in alfalfa by regulating Fe acquisition and antioxidant defense. Antioxidants, 10 (10), 1556. https://doi.org/10.3390/antiox10101556

Rai, S., Singh, P.K., Mankotia, S., Swain, J., Satbhai, S.B., 2021. Iron homeostasis in plants and its crosstalk with copper, zinc, and manganese. Plant Stress, 1, 100008. https://doi.org/10.1016/j.stress.2021.100008

Ramakrishna, B., Rao, S.S.R., 2013. Preliminary studies on the involvement of glutathione metabolism and redox status against zinc toxicity in radish seedlings by 28-Homobrassinolide. Environ. Exp. Bot., 96, 52–58. https://doi.org/10.1016/j.envexpbot.2013.08.003

Ramírez, L., Bartoli, C.G., Lamattina, L., 2013. Glutathione and ascorbic acid protect *Arabidopsis* plants against detrimental effects of iron deficiency. J. Exp. Bot., 64 (11), 3169–3178. https://doi.org/10.1093/jxb/ert153

Ramos, S.J., Rutzke, M.A., Hayes, R.J., Faquin, V., Guilherme, L.R.G., Li, L., 2011. Selenium accumulation in lettuce germplasm. Planta 233, 649–660. https://doi.org/10.1007/s00425-010-1323-6

Ranieri, A., Castagna, A., Baldan, B., Soldatini, G.F., 2001. Iron deficiency differently affects peroxidase isoforms in sunflower. J. Exp. Bot., 52 (354), 25–35. https://doi.org/10.1093/jexbot/52.354.25

Santos, C.S., Ozgur, R., Uzilday, B., Turkan, I., Roriz, M., Rangel, A.O.S.S, Carvalho, S.M.P., Vasconcelos, M.W., 2019. Understanding the role of the antioxidant system and the tetrapyrrole cycle in iron deficiency chlorosis. Plants, 8 (9), 348. https://doi.org/10.3390/plants8090348

Sarruge, J.R., Haag, H.P., 1974. *Análises químicas em plantas* (p. 56). Piracicaba: Esalq.

Schiavon, M., Pilon-Smits, E.A., 2017. The fascinating facets of plant selenium accumulation–biochemistry, physiology, evolution and ecology. New Phytologist, 213 (4), 1582–1596. https://doi.org/10.1111/nph.14378

Shanmugam, V., Wang, Y. W., Tsednee, M., Karunakaran, K., Yeh, K. C., 2015. Glutathione plays an essential role in nitric oxide-mediated iron-deficiency signaling and iron-deficiency tolerance in *Arabidopsis*. Plant J., 84 (3), 464–477. https://doi.org/10.1111/tpj.13011

Shi, J., Fu, X.Z., Peng, T., Huang, X.S., Fan, Q.J., Liu, J.H., 2010. Spermine pretreatment confers dehydration tolerance of citrus in vitro plants via modulation of antioxidative capacity and stomatal response. Tree Physiology, 30 (7), 914–922. https://doi.org/10.1093/treephys/tpq030

Silva, L.C.C., Mayrink, D.B., Bueno, R.D., Piovesan, N. D., Ribeiro, C., 2022. Reference genes and expression analysis of seed desaturases genes in soybean mutant accessions. Biochem Genet, 60, 937–952. https://doi.org/10.1007/s10528-021-10135-x

Solti, Á., Müller, B., Czech, V., Sárvári, É., Fodor, F., 2014. Functional characterization of the chloroplast ferric chelate oxidoreductase enzyme. New Phytologist, 202 (3), 920–928. https://doi.org/10.1111/nph.12715

Takeda, T., Ishikawa, T., Shigeoka, S., 1997. Metabolism of hydrogen peroxide by the scavenging system in *Chlamydomonas reinhardtii*. Physiol. Plant., 99 (1), 49–55. https://doi.org/10.1111/j.1399-3054.1997.tb03429.x

Therby-Vale, R., Lacombe, B., Rhee, S.Y., Nussaume, L., Rouached, H., 2021. Mineral nutrient signaling controls photosynthesis: focus on iron deficiency-induced chlorosis. Trends Plant Sci., 27 (5), 502–509. https://doi.org/10.1016/j.tplants.2021.11.005

Tomasi, N., Mimmo, T., Terzano, R., Alfeld, M., Janssens, K., Zanin, L., Pinton, R., Varanini, Z., Cesco, S., 2014. Nutrient accumulation in leaves of Fe-deficient cucumber plants treated with natural Fe complexes. Biol Fertil Soils, 50 (6), 973–982. https://doi.org/10.1007/s00374-014-0919-6

Waters, B.M., Amundsen, K., Graef, G., 2018. Gene expression profiling of iron deficiency chlorosis sensitive and tolerant soybean indicates key roles for phenylpropanoids under alkalinity stress. Front. Plant Sci., 9, 10. https://doi.org/10.3389/fpls.2018.00010

Waters, B.M., McInturf, S.A., Stein, R.J., 2012. Rosette iron deficiency transcript and microRNA profiling reveals links between copper and iron homeostasis in *Arabidopsis thaliana*. J. Exp. Bot., 63 (16), 5903–5918. https://doi.org/10.1093/jxb/ers239

Xiao, M., Li, Z., Zhu, L., Wang, J., Zhang, B., Zheng, F., Zhao, B., Zhang, H., Wang, Y., Zhang, Z., 2021. The multiple roles of ascorbate in the abiotic stress response of plants: antioxidant, cofactor, and regulator. Front. Plant Sci., 12, 598173. https://doi.org/10.3389/fpls.2021.598173

Xie, X., Hu, W., Fan, X., Chen, H., Tang, M., 2019. Interactions between phosphorus, zinc, and iron homeostasis in nonmycorrhizal and mycorrhizal plants. Front. Plant Sci., 10, 1172. https://doi.org/10.3389/fpls.2019.01172

Yildiztugay, E., Ozfidan-Konakci, C., Kucukoduk, M., Tekis, S.A., 2017. The impact of selenium application on enzymatic and non-enzymatic antioxidant systems in *Zea mays* roots treated with combined osmotic and heat stress. Archives of Agronomy and Soil Science, 63 (2), 261–275. https://doi.org/10.1080/03650340.2016.1201810

Ylivainio, K. (2010) Effects of iron(III) chelates on the solubility of heavy metals in calcareous soils. Environmental Pollution, 158, 3194–3200. https://doi.org/10.1016/j.envpol.2010.07.004

Yoshida, C.H.P., Pacheco, A.C., Lapaz, A.M., Ferreira, C.S., Dal-Bianco, M., Viana, J.M.S., Ribeiro C., 2023. Tolerance mechanisms to aluminum in popcorn inbred lines involving aluminum compartmentalization and ascorbate–glutathione redox pathway. Planta, 257 (2), 28. https://doi.org/10.1007/s00425-022-04062-3

Zhao, J., Zhang, W., Qiu, Q., Meng, F., Zhang, M., Rao, D., Wang, Z., Yan, X., 2018. Physiological regulation associated with differential tolerance to iron deficiency in soybean. Crop Sci., 58 (3), 1349–1359. https://doi.org/10.2135/cropsci2017.03.0154

Zheng, L., Huang, F., Narsai, R., Wu, J., Giraud, E., He, F., Cheng, L., Wang, F., Wu, P., Whelan, J., Shou, H., 2009. Physiological and transcriptome analysis of iron and phosphorus interaction in rice seedlings. Plant Physiol., 151 (1), 262–274. https://doi.org/10.1104/pp.109.141051

Zheng, X., Gong, M., Zhang, Q., Tan, H., Li, L., Tang, Y., Li, Z., Peng, M., Deng, W., 2022. Metabolism and regulation of ascorbic acid in fruits. Plants, 11 (12), 1602. https://doi.org/10.3390/plants11121602

Zocchi, G., De Nisi, P., Dell'Orto, M., Espen, L., Gallina, P.M., 2007. Iron deficiency differently affects metabolic responses in soybean roots. J. Exp. Bot., 58 (5), 993–1000. https://doi.org/10.1093/jxb/erl259

Material supplementary

Table S1. Superoxide dismutase subfamily grouping and primer sequences used in this study.

Clusters	Genes	Forward primer	Reverse primer
Cu/Zn-SOD1	*Glyma.03G242900* *Glyma.19G240400*	GGACACTACCAATGGTTGCCT	ACATTAACATTCCCAAGATCACC
Cu/Zn-SOD2	*Glyma.11G192700* *Glyma.12G081300* *Glyma.12G178800*	TGACCTGGGAAACATAGTTGC	TTTCCAAGGTCATCCTCAAGC
Cu/Zn-SOD3	*Glyma.16G153900*	CGGAGACAACAACATTAGAGG	TGGAGTTGCAGCCATTGGTG
Fe-SOD1	*Glyma.02g087700.1* *Glyma.10G117100* *Glyma.10G193500* *Glyma.20G196900*	AATAAGGGTGACATTCTTCCAG	ACTCCCAGAAGAAGTCATGGT
Fe-SOD2	*Glyma.20G050800*	GCCATTTGCCCAATTGTGTGG	AGCCTCTGCTCTTGTCAATCG
Mn-SOD1	*Glyma.04g221300.1* *Glyma.06g144500.1*	TCTGGATTACGACTATGGCGC	GTGATGTAAGTCTGGTGGTGC

Material supplementary

Table S2. Fe/Cu ratio, Fe/Zn ratio, and Fe/Mn ratio in soybean leaves at the V3 phenological stage. Soybean plants were subjected to absence (0 µM), insufficiency (10 µM), and sufficiency of iron (45 µM) for 9 days, associated with the absence (0 µM) or presence of sodium selenate (10 µM), with the beginning of the Se supply 3 days before the imposition of Fe deficiency.

Traits	Fe absence		Fe insufficiency		Fe sufficiency	
	-Se	+Se	-Se	+Se	-Se	+Se
	No unity					
Fe/Cu ratio	3.48E ± 4.5	6.34D ± 7.4	16.02C ± 2.9	15.93C ± 7.1	19.03B ± 3.1	22.97A ± 4.1
Fe/Zn ratio	0.32D ± 4.5	0.72C ± 4.5	1.70B ± 4.5	1.52B ± 4.5	2.45A ± 4.5	2.44A ± 4.5
Fe/Mn ratio	0.10E ± 17.3	0.30D ± 24.5	0.66B ± 20.3	0.54C ± 34.7	1.03A ± 20.8	0.95A ± 32.8

Different letters indicate significant differences according to Scott-Knott's test ($p < 0.05$). ± means standard error ($n = 5$ plants).

Article II

Theor. Exp. Plant Physiol.
https://doi.org/10.1007/s40626-024-00330-7

Positive modulation of selenium on photosynthetic performance in soybean under iron depletion

Allan de Marcos Lapaz · Camila Hatsu Pereira Yoshida · Daniel Gomes Coelho · Wagner Luiz Araujo · Maximiller Dal-Bianco · Cleberson Ribeiro

https://doi.org/10.1007/s40626-024-00330-7

Abstract: Although iron (Fe) is abundant in most agricultural soils, its bioavailability to plants is limited. The Fe deficiency can cause significant changes in plant metabolites, impacting the plant's life cycle. In this context, selenium (Se) has been shown promising effects against Fe deficiency. However, there are still few studies addressing the role of Se against the deleterious effects of Fe deficiency, mainly with the soybean crop. Hence, this study aimed to evaluate the effects of Se on dry mass, Fe concentration in the roots and shoots, as well as to assess the photosynthetic performance and primary metabolism in soybean plants subjected to Fe deficiency. The experimental design used was completely randomized with 4 treatments: 1) absence of Fe without Se; 2) absence of Fe with Se; 3) sufficiency of Fe without Se (control); and 4) sufficiency of Fe with Se. Our results demonstrated that Fe deficiency significantly reduced shoot and root dry mass, as well as Fe concentration in plants. However, supplementation with Se effectively mitigated this reduction in dry mass. Additionally, Fe deficiency had a detrimental impact on photosynthetic traits, whereas Se-treated plants exhibited a higher net CO_2 assimilation rate and improved carboxylation efficiency. Moreover, Fe deficiency negatively influenced primary metabolism, leading to the altered accumulation of sugars and amino acids and reduced protein concentration. In contrast, Se-treated plants showed lower accumulation of sucrose and starch and maintenance of protein concentration.These findings highlight the potential of Se as a valuable intervention to mitigate Fe deficiency in soybean crops.

Keywords: *Glycine max* L. Iron translocation factor. Photosynthetic performance. Primary metabolism.

1. Introduction

The bioavailability of iron (Fe) to plants is limited even in most Fe-rich agricultural soils (Lei et al. 2014; Kobayashi et al. 2019). Under natural conditions, Fe^{3+} can precipitate in the form of Fe oxides and oxy-hydroxides, or, more commonly, as Fe^{2+}, interacting with the various minerals present in the soil (Gattullo et al. 2018).

The manifestation of interveinal chlorosis and reduction in biomass are the most common symptoms observed in plants cultivated in Fe-poor environments (Mamidi et al. 2011; Kaya et al. 2019; He et al. 2023). Since the chloroplast is the organelle that holds the highest amount of Fe in the leaf (Terry and Low, 1982), the deficiency of this metal severely affects photosynthesis (He et al. 2023). It also impacts other Fe-dependent physiological processes in the chloroplast, such as the activity of the chlorophyll *a* oxygenase enzyme and TIC 55 (TRANSLOCON OF INNER CHLOROPLAST ENVELOPE 55) (Solti et al. 2012).

Due to the negative impact of Fe deficiency on both the photochemical and biochemical steps of photosynthesis (Wang et al. 2017; He et al. 2023), the plant's metabolic processes are severely compromised. This includes disruptions in energy flow, impaired metabolism of organic compounds such as carbohydrates, lipids, amino acids, nucleic acids, and vitamins, as well as imbalances in nutrient status and the elimination of metabolic waste (Zhang et al. 2019). As a result of these alterations, crop yield can be significantly impaired (Álvarez-Fernández et al. 2011).

Several studies have demonstrated the ability of selenium (Se) to enhance photosynthetic pigments concentration (Cunha et al. 2022), improve photosynthetic rates (Yin et al. 2019), modulate nitrogen (N) and carbohydrate metabolism (Cunha et al. 2022; Cunha et al. 2023), and reduce oxidative stress (Cunha et al. 2022). However, few studies have assessed the effects of Se on Fe-deficient plants. Hajiboland et al. (2020) examined Se supplementation in Fe-restricted rapeseed plants and observed an increase in chlorophyll concentration, photosynthetic rate, photochemical traits, and cytoplasmic pool concentration of Fe^{2+}. Furthermore, Lapaz et al. (2023) found that Se alleviated leaf chlorosis, influenced the expression of genes involved in superoxide dismutase (SOD) isoform synthesis, and improved glutathione (GSH) metabolism in Fe-restricted soybean.

Soybean [*Glycine max* (L.) Merrill] is considered one of the most important legumes in the world for human and animal nutrition (Ibañez et al. 2020), being extensively cultivated for food production (Haque et al. 2022). The grains of soybean generally have high protein concentration (42%) and oil concentration (22%) (Haque et al. 2022; Rahman et al. 2022). However, soybean is sensitive to Fe deficiency (Gonzalo et al. 2013; Santos et al. 2021). Therefore, studies focused on improving physiological and metabolic traits are essential to mitigate productivity losses in this crop.

Here, we hypothesize that the supply of Se can enhance the photosynthetic performance and metabolic pathways of soybean plants exposed to Fe deficiency, resulting in increased dry mass

accumulation. Therefore, the objectives of this study were to evaluate the effects of Se on dry mass, Fe concentration in the roots and shoots, as well as to assess the photosynthetic performance and primary metabolism in soybean plants subjected to Fe deficiency.

2. Material and Method

2.1. Plant material and experimental conditions

The experiment was conducted at the Universidade Federal de Viçosa. Initially, soybean seeds of the cultivar 'Raio' were disinfected with 1% NaOCl (v/v) for 3 min and then washed with deionized water. The seeds were placed on paper rolls, moistened with 100 µM $CaCl_2$ (pH 7.0), and incubated in a cultivation chamber. They were then conditioned in the dark at 25°C for 3 days, followed by exposure to light for another 3 days.

On the seventh day, seedlings were acclimated in polypropylene pots with 2 L containing half-strength Clark's solution (pH 5.5) (Clark 1975) for 2 days. The nutrient solution consisted of the following concentrations and sources: 0.5 mM NH_4NO_3, 0.52 mM $Ca(NO_3)_2 \cdot 4H_2O$, 0.4 mM KNO_3, 0.0345 mM $KH_2PO_4 \cdot 2H_2O$, 0.465 mM KCl, 0.3 mM $MgSO_4 \cdot 7H_2O$, 22.5 µM Fe-EDTA, 9.5 µM H_3BO_3, 3.5 µM $MnCl_2 \cdot 4H_2O$, 1 µM $ZnSO_4 \cdot 7H_2O$, 0.3 µM $Na_2MoO_4 \cdot 4H_2O$, and 0.25 µM $CuSO_4 \cdot 5H_2O$. The plants were maintained in a cultivation chamber under continuous aeration with a temperature of 25 ± 1°C, light intensity at 200 µmol photons m^{-2} s^{-1} relative humidity maintained at 80%, and a light/dark cycle of 16/8 h.

On the ninth day, the plants were divided into 2 groups: absence (0 mM) and presence (10 µM) of sodium selenate (Na_2SeO_4) (Hajiboland et al. 2020; Lapaz et al. 2023) in the total-strength Clark's solution (pH 6.0) (Clark 1975) for 3 days. Posteriorly, the seedlings already at the V1 stage (Fehr et al. 1971) were exposed to absence (0 µM) and sufficiency (45 µM) of Fe (applied as Fe-EDTA), associated with the absence and presence of Se for 9 days. The nutrient solution was renewed every 3 days, with the pH adjusted daily to 6.0.

After that period, coinciding with the V3 stage (Fehr et al. 1971), the first fully expanded trifoliate leaf (counting from the apex) was used to investigate photosynthetic performance and then collected for determination of biometric traits and for laboratory analysis, which was frozen in liquid N_2 and stored at −80ºC.

2.2. Soybean dry mass and quantification of Fe concentration

The shoot and root of each plant were oven dried at 65°C for 72 h and ground in a Wiley-type mill. After determination of shoot and root dry mass, the material was used to determine Fe concentration. For such, the dried material was digested in HNO_3–$HClO_4$ (4:1, v/v) at 200°C. The

measurements were carried out in an inductively coupled plasma optical emission spectrophotometer (ICP-OES, Optima 8300 DV, Perkin Elmer, Waltham, USA). A standard Fe solution was used to calibrate the curve. Blank reagent samples were also used in digestion for quality control (Sarruge and Haag, 1974).

2.3. Gas exchanges analysis and chlorophyll a fluorescence analysis

The gas exchange and fluorescence evaluations of chlorophyll *a* were performed simultaneously using a portable infrared gas analyzer (LI-6400XT, LI-COR, Lincoln, NE, USA) equipped with an integrated fluorescence chamber (6400-40 LCF, Li-Cor) in the central leaflet of the first fully expanded trifoliate leaf. Conditions in the leaf chamber were adjusted to 1,000 μmol photons m^{-2} s^{-1} (10% blue and 90% red), 400 μmol CO_2 mol^{-1} air, 300 μmol s^{-1} of flow rate, and natural vapor pressure deficit (ranging from 1.2 to 1.8 kPa) during gas exchange measurements (Toral-Juárez et al. 2021). The following traits were measured: net CO_2 assimilation rate (A), stomatal conductance (gs), transpiration rate (E), internal CO_2 concentration (Ci), and carboxylation efficiency (EiC, A/Ci).

Initially, for chlorophyll *a* fluorescence evaluation, the plants were previously dark-adapted (30 min), then the central leaflet was illuminated with weak modulated measuring beams (0.03 μmol m^{-2} s^{-1}) followed by pulses of saturated white light (8,000 μmol m^{-2} s^{-1}; 0.8 s), to determine the minimum and maximum fluorescence (F_0 and F_m, respectively) and maximum efficiency of PSII photochemistry (F_v/F_m) = [(F_m – F_0)/F_m)]. Immediately afterwards, the steady-state fluorescence yield (F_s) was measured after recording the gas exchange parameters using an actinic PPFD of 1,000 μmol m^{-2} s^{-1}. Subsequently, a saturating white light pulse (8,000 μmol m^{-2} s^{-1}; 0.8 s) was applied to achieve the light-acclimated maximum fluorescence (F_m'). Following this light pulse, a far-red illumination was applied to measure the initial fluorescence (F_0'). After these steps, the following traits were obtained: excitation energy capture efficiency of PSII reaction centers F_v'/F_m' = (F_m' – F_0')/F_m'), effective PSII quantum yield (ΦPSII) = (F_m' – F_s)/F_m', photochemical quenching (q_P) = (F_m' – F_s)/(F_m – F_0'), non-photochemical quenching (NPQ) = (F_m/F_m') – 1, and apparent electron transport rate (ETR) = ΦPSII × PPFD × f × α (Maxwell and Johnson 2000).

2.4. Extraction of primary metabolites

After the lyophilization process, the first fully expanded trifoliate leaf (10 mg) were homogenized and subjected to methanolic extraction (Lisec et al. 2006). Subsequently, the glucose, fructose, sucrose, fumarate, malate, ammonia, total amino acid, and proline concentrations were

quantified from the soluble fraction, whereas the starch and total protein concentrations were quantified from the insoluble fraction.

2.5. Quantification of protein, starch, glucose, fructose, and sucrose concentrations

The insoluble fraction (pellet) was resuspended in 0.1 M NaOH and incubated for 1 h at 95°C under agitation at 750 rpm (Cross et al. 2006). Subsequently, the samples were centrifuged at 13,500 rpm at 25°C for 10 min. Lastly, 5 µL of the supernatant (10× diluted) was added to a microplate containing 250 µL of Bradford reagent (Bradford, 1976). The mixture was kept in the dark for 10 min, and absorbance was measured at 595 nm using a microplate reader (Tecan, Infinite M200 PRO, Männedorf, Switzerland). The determination of total protein concentration was measured using a calibration curve containing bovine serum albumin (BSA) as a standard.

To determine the starch concentration, the resuspended fraction was neutralized with 1 M acetic acid. Next, samples were kept overnight at 37°C in a reaction medium to hydrolyze the starch. The reaction contained 29.5 mM sodium acetate (pH 4.9), 0.17 U amyloglucosidase, 0.004 U α-amylase, and 10 µL of extract (final volume = 100 µL). After centrifugation at 10.000 rpm for 15 s, a reaction medium was prepared containing 714.3 mM HEPES/KOH (pH 7.0) buffer, 2.14 mM $MgCl_2$, 2.4 mM ATP, 1.1 mM $NADP^+$, 0.54 U glucose-6-phosphate dehydrogenase (G6PDH), and 10 µL of extract (final volume = 210 µL). After the optical density (OD) stabilization, 1.5 U hexokinase was added per reaction (Fernie et al. 2001). The reduction of $NADP^+$ was measured at 340 nm using a microplate reader, at 1-min intervals. To determine glucose, fructose, and sucrose concentrations, an aliquot of the soluble fraction was added to a reaction medium. The reaction contained 71.4 mM HEPES/KOH (pH 7.0) buffer, 2.14 mM $MgCl_2$, 2.4 mM ATP, 1.1 mM $NADP^+$, 0.54 U G6PDH, and 25 µL of extract (final volume = 210 µL). The reduction of $NADP^+$ was recorded at 340 nm using a microplate reader, at 1-min intervals. After the OD stabilization, the following enzymes were added per reaction: 1.5 U hexokinase, 0.7 U phosphoglucose isomerase, and 5 U invertase (Fernie et al. 2001); intervals were 20 min between each application. To calculate the sugars concentrations, the following equation was used: NADPH (µmol) = $\Delta OD / (2.85 \times 6.22)$.

2.6. Quantification of fumarate and malate concentrations

Fumarate and malate concentrations were determined as described by Nunes-Nesi et al. (2007). Initially, a reaction medium containing 0.1 M Tricine/KOH buffer (pH 9.0), 5 mM $MgCl_2$, 1 mM MTT (methylthiazolyldiphenyl-tetrazolium bromide), 3 mM NAD^+, 0.4 mM PES (phenazine ethosulfate), 0.5% Triton X100 (v/v), and 3 µL of extract (final volume = 100 µL). The absorbance was read at 570 nm using a microplate reader, at 1-min intervals. After the OD stabilization, the

following enzymes were added per reaction: 1 U malate dehydrogenase and 0.1 U fumarase; intervals were 20 min between each application. To calculate the fumarate and malate concentrations, the rate of change in their absorbances was compared with that of fumarate and malate standards, respectively.

2.7. Quantification of ammonia concentration

The ammonia concentration was determined using the method described by McCullough (1967). Briefly, a reaction medium containing 48.3 mM phenol, 0.077 μM sodium nitroprusside (SNP), 56.8 mM sodium hydroxide, 68 mM disodium phosphate, 2.3% sodium hypochlorite (w/v), and 20 μL of extract (final volume = 220 μL) was added to the microplate and incubated for 60 min at 37°C. The ammonia concentration was determined based on the calibration curve using ammonium sulfate standard.

2.8. Quantification of proline and total amino acid concentrations

To determine the proline concentration, a reaction medium containing 50 μL of extract (12× concentrated), 0.66% ninhydrin (w/v), 40% acetic acid (v/v), and 13.3% ethanol (v/v) (final volume = 150 μL) was heated at 95ºC for 20 min and measured the absorbance at 520 nm (Carillo and Gibon, 2011). The proline concentration was calculated based on the authentic proline standard curve.

Total amino acid concentration was determined as described by Cross et al. (2006). Briefly, a reaction medium containing 250 mM citrate buffer (pH 5.2), 0.05% ascorbic acid (w/v), 0.5% ninhydrin (dissolved in 70% ethanol; w/v), and 50 μL of extract (final volume = 200 μL) was added to the microplate and incubated for 20 min at 95°C. Lastly, absorbance was read at 570 nm using a microplate reader. The total amino acid concentration was determined based on the calibration curve using leucine standards.

2.9. Experimental design and statistical analysis

The experimental design used was completely randomized with 4 treatments: 1) absence of Fe without Se; 2) absence of Fe with Se; 3) sufficiency of Fe without Se (control); and 4) sufficiency of Fe with Se. The experiment was carried out with 5 replications containing 4 plants in each pot. Each plant constituted 1 experimental unit.

Normality and homoscedasticity of the data were verified using the Shapiro-Wilk's and Bartlett's tests, respectively, both at 0.05 significance level. Then, the data were subjected to analysis of variance (ANOVA) using the F test ($p \leq 0.05$). When significant, the traits were subjected to the

Duncan's test ($p < 0.05$). As supplementary analysis, principal component analysis (PCA) was performed using 'FactoMineR', 'factoextra', and 'ggplot2' packages. All statistical analysis was performed in the R software (R Development Core Team, 2019).

3. Results

The shoot and root dry mass decreased by 7 and 13%, respectively, in plants exposed to the absence of Fe without Se, but did not differ from those exposed to the absence of Fe with Se (Fig. 1a, d). Fe concentration in the shoot and root was respectively lower by 38 and 60% in the absence of Fe (Fig. 1b, e). Furthermore, the highest Se concentration was observed in the root and shoot of Se-supplemented plants (Fig. 1c, f).

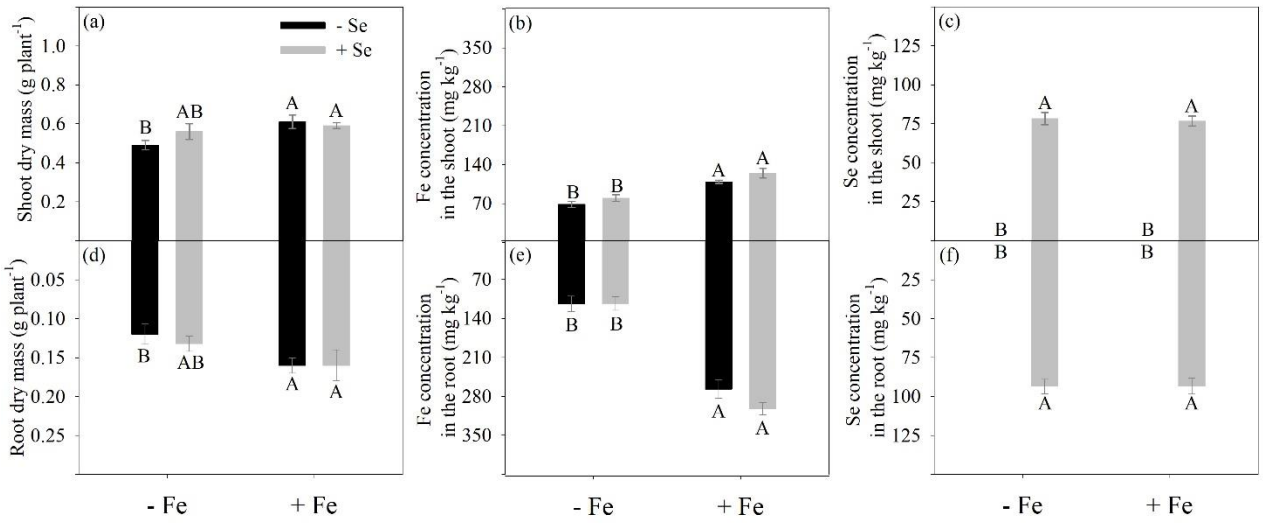

Figure 1. Shoot dry mass (a), Fe concentration in the shoot (b), Se concentration in the shoot (c), root dry mass (d), Fe concentration in the root (e), and Se concentration in the root (f) in soybean at the V3 phenological stage. Soybean plants were exposure to the nutrient solution with absence (–Fe) and sufficiency of iron (45 µM; +Fe) for 9 days, associated with the absence (0 µM) or presence of sodium selenate (10 µM), with the beginning of the Se supply 3 days before the imposition of Fe deficiency. Different letters indicate significant differences according to Duncan's test ($p < 0.05$). Bars represent the standard error ($n = 5$ plants).

The gas exchange traits A, g_s, E, and EiC decreased in the plants exposed to the absence of Fe (Fig. 2a–c, e). However, for A and EiC, the decrease was lower in plants treated with Se (Fig. 2a, e). On the other hand, Ci was higher in plants exposed to the absence of Fe without Se, but did not differ from those exposed to the absence of Fe with Se (Fig. 2d).

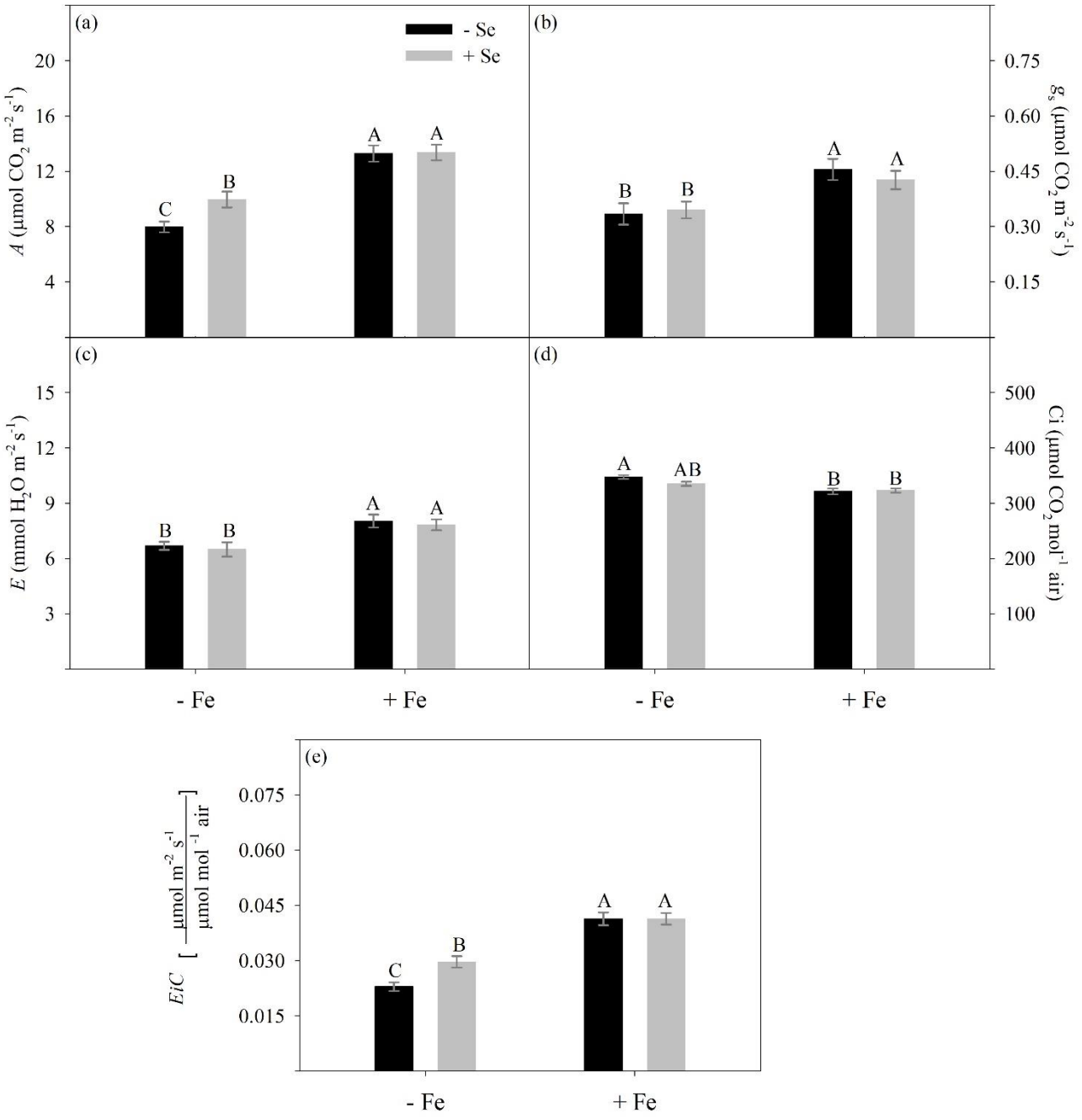

Figure 2. Net photosynthetic rate (*A*, a), stomatal conductance (g_s, b), transpiration rate (*E*, c), intercellular CO_2 concentration (Ci, d), and carboxylation efficiency (EiC, e) in soybean leaves at the V3 phenological stage. Soybean plants were exposure to the nutrient solution with absence (–Fe) and sufficiency of iron (45 µM; +Fe) for 9 days, associated with the absence (0 µM) or presence of sodium selenate (10 µM), with the beginning of the Se supply 3 days before the imposition of Fe deficiency. Different letters indicate significant differences according to Duncan's test ($p < 0.05$). Bars represent the standard error ($n = 5$ plants).

The traits photochemical F_v/F_m, F_v'/F_m', Φ_{PSII}, ETR, and q_P decreased in the absence of Fe, with the highest decreases in the plants without Se (Fig. 3a–e). Additionally, there was a reduction in NPQ only in plants exposed to the absence of Fe with Se (Fig. 3f).

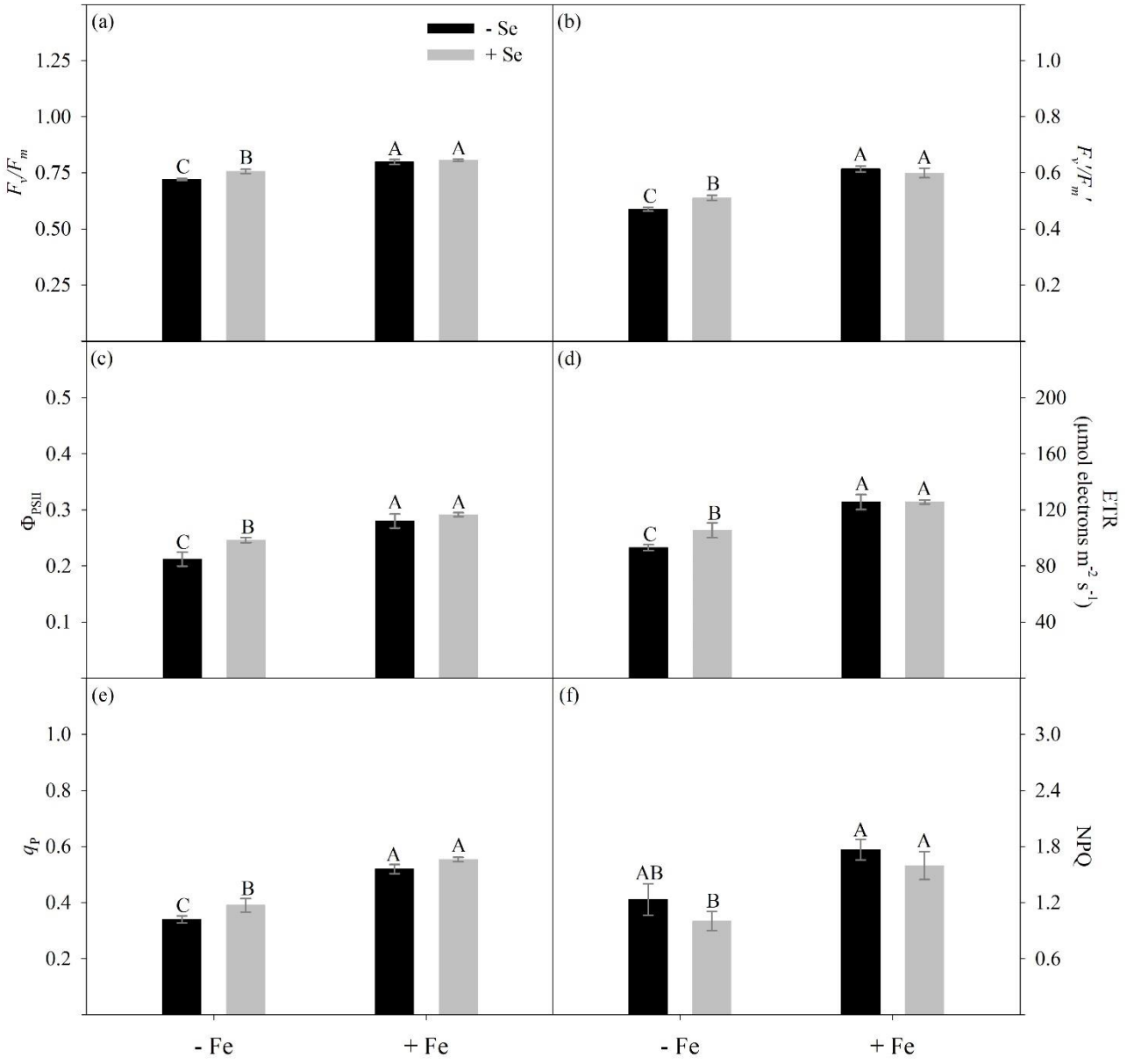

Figure 3. Maximum efficiency of PSII photochemistry (F_v/F_m, a), excitation energy capture efficiency of PSII reaction centers (F_v'/F_m', b), effective PSII quantum yield (Φ_{PSII}, c), electron transport rate (ETR, d), photochemical quenching (q_P, e), and non-photochemical quenching (NPQ, f) in soybean leaves at the V3 phenological stage. Soybean plants were exposure to the nutrient solution with absence (–Fe) and sufficiency of iron (45 µM; +Fe) for 9 days, associated with the absence (0 µM) or presence of sodium selenate (10 µM), with the beginning of the Se supply 3 days before the imposition of Fe deficiency. Different letters indicate significant differences according to Duncan's test ($p < 0.05$). Bars represent the standard error ($n = 5$ plants).

The glucose, fructose, fumarate, and malate concentrations were not different for any of the studied situations (Fig. 4a–b, e–f). However, plants submitted to the absence of Fe showed an increase in sucrose (absence and presence of Se) and starch (absence of Se) concentrations (Fig. 4c–d). The increase in sucrose concentration was more pronounced in plants exposed to the absence of Fe without Se, with a 12% increase (Fig. 4c).

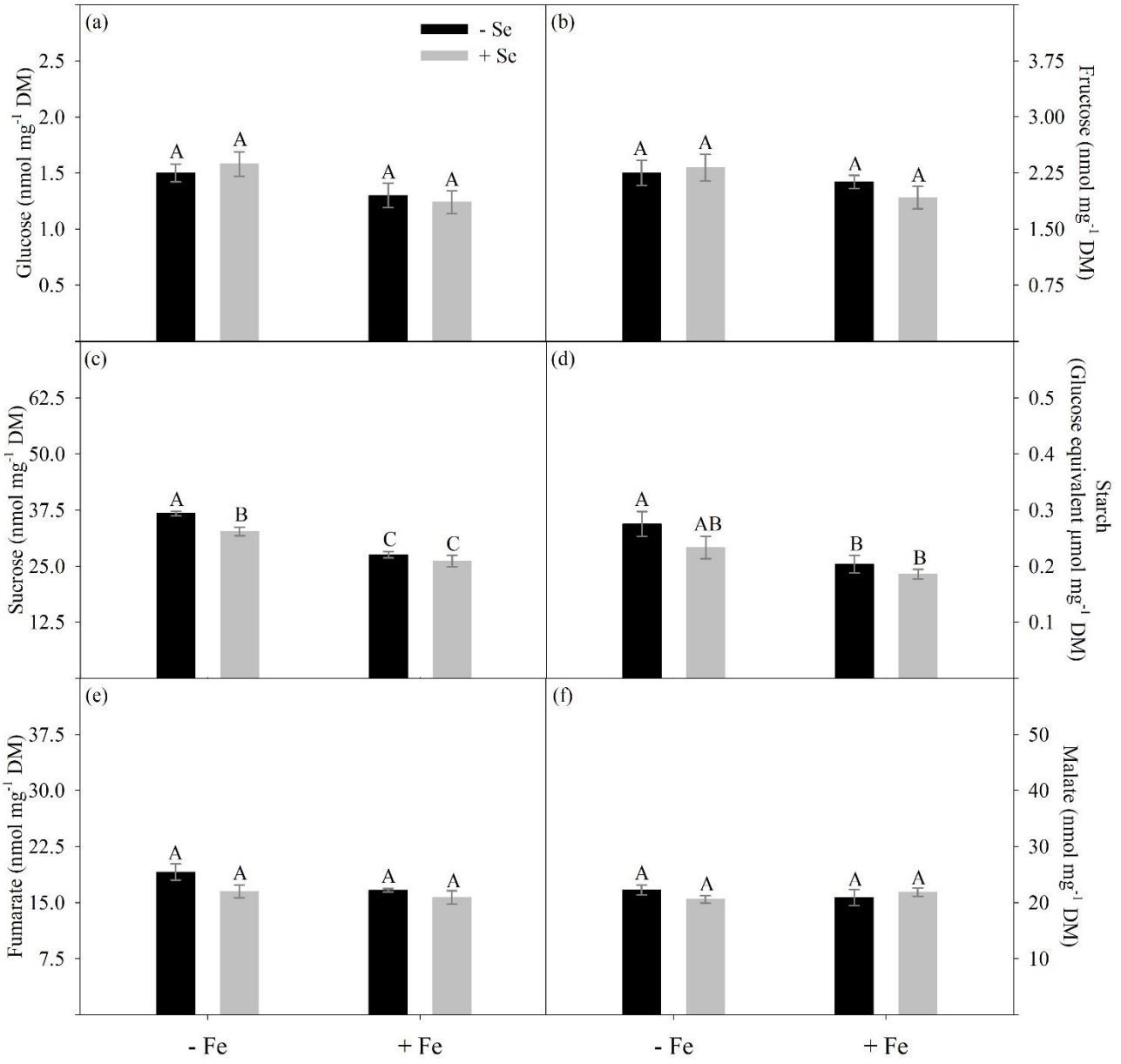

Figure 4. Glucose (a), fructose (b), sucrose (c), starch (d) fumarate (e), and malate (f) concentration in soybean leaves at the V3 phenological stage. Soybean plants were exposure to the nutrient solution with absence (–Fe) and sufficiency of iron (45 µM; +Fe) for 9 days, associated with the absence (0 µM) or presence of sodium selenate (10 µM), with the beginning of the Se supply 3 days before the imposition of Fe deficiency. Different letters indicate significant differences according to Duncan's test ($p < 0.05$). Bars represent the standard error ($n = 5$ plants). Abbreviation: DM = dry mass.

In plants exposed to the absence of Fe, the total amino acid and proline concentrations increased in both the absence and presence of Se (Fig. 5a, c). In contrast, the total protein concentration decreased only in the absence of Fe without Se (Fig. 5b). The ammonia concentration decreased in plants exposed to the absence of Fe (absence and presence of Se) and Fe sufficiency (presence of Se), as shown in Figure 5d.

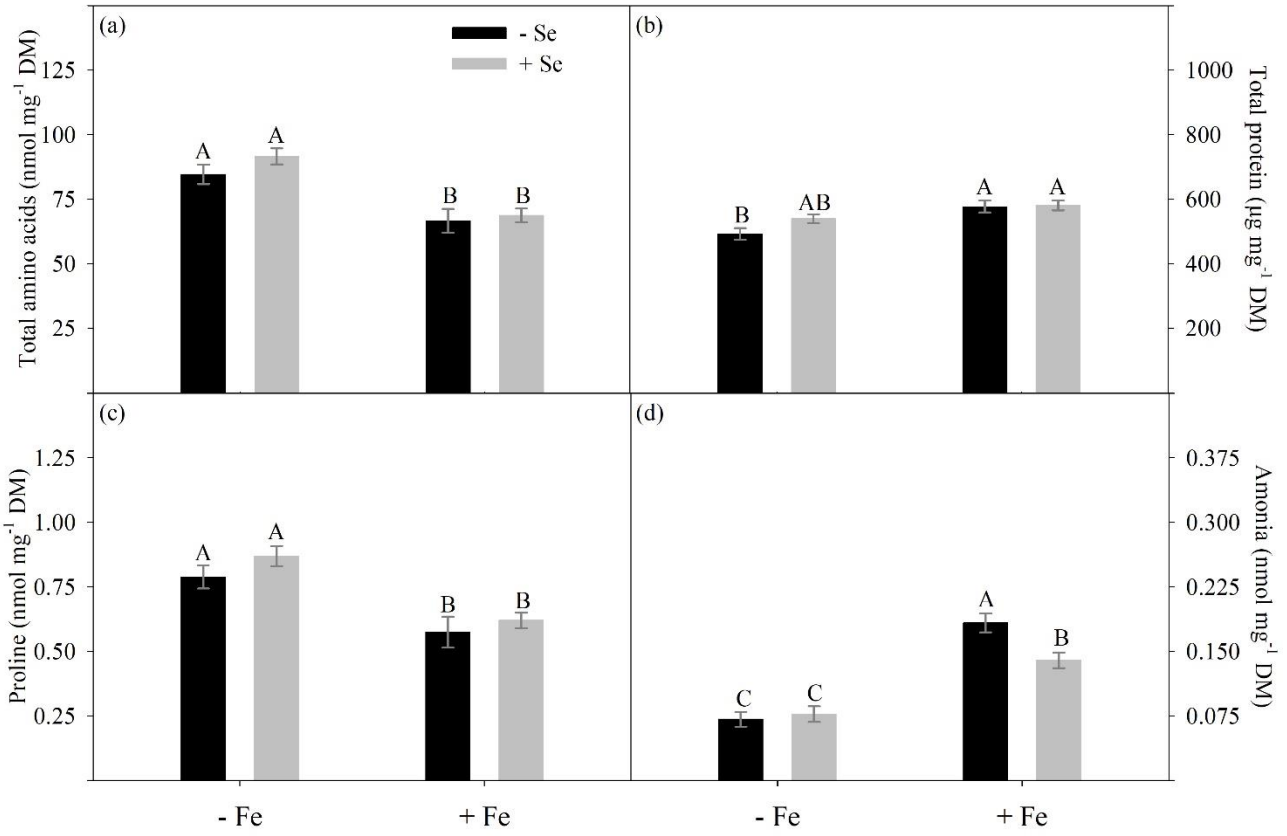

Figure 5. Total amino acids (a), total protein (b), proline (c), and ammonia (d) concentration in soybean leaves at the V3 phenological stage. Soybean plants were exposure to the nutrient solution with absence (–Fe) and sufficiency of iron (45 µM; +Fe) for 9 days, associated with the absence (0 µM) or presence of sodium selenate (10 µM), with the beginning of the Se supply 3 days before the imposition of Fe deficiency. Different letters indicate significant differences according to Duncan's test ($p < 0.05$). Bars represent the standard error ($n = 5$ plants). Abbreviation: DM = dry mass.

4. Discussion

Into the cell, the Fe can interact with various organic substances and act as a structural and functional component, including the heme group, cytochromes, Fe-S clusters, and ferredoxin (Kroh and Pilon 2020). Since these components play a key role in the electron transport chain, both the photosynthetic and respiratory systems can be substantially affected under Fe deficiency (Hantzis et al. 2018; He et al. 2023), resulting in reduced plant growth and development (Álvarez-Fernández et al. 2011; Hantzis et al. 2018).

The decrease in shoot and root dry mass in plants exposed to the absence of Fe without Se, corroborates with the results found by other studies with strawberry (Kaya et al. 2019), oilseed rape (Hajiboland et al. 2020), and soybean (He et al. 2023). However, the negative impact of Fe deficiency on these traits was mitigated by the Se addition, as observed by Hajiboland et al. (2020), suggesting a beneficial role of Se against the negative effects of Fe deficiency in plants.

As the leaf is a plant organ with a high demand for Fe (Kroh and Pilon, 2020), especially within the chloroplasts (Li et al. 2021), the reduction in Fe concentration in the shoot caused the decline in soybean photosynthetic performance (Fig 2–3). However, with the Se supply, the changes in *A*, Ci, and EiC in the absence of Fe were less pronounced (Fig. 2a, d–e, and S1), suggesting a lesser biochemical limitation in plants treated with Se compared to those without Se.

The main positive effects of Se observed in the present work were in gas exchange traits (*A* and EiC) (Fig. 2a, e) and in photochemical traits (Fig. 3 and S1). Se supply provided to an increase in F_v/F_m, reaching a value of 0.76 (Fig. 3a and S1), which is considered suitable for most species, ranging from 0.75 to 0.85 (Peña Calzada et al. 2014). On the other hand, plants cultivated without Se exhibited a value of 0.72, indicating a potential onset of PSII photoinhibition. Se also attenuated the F_v'/F_m' reduction, possibly due to the increase in photosynthetic pigment concentration reported by Lapaz et al. (2023), reflecting in increased values of Φ_{PSII}, ETR, and q_P compared to plants not treated with Se (Fig. 3c–e and S1). Therefore, these adjustments conferred a higher light-harvesting capacity to the plant, as well as increased fluorescence dissipation and electron transport processes in the chloroplasts and subsequent generation of ATP and NADPH (Wang et al. 2017; He et al. 2023), which may explain the observed increase in *A* (Fig. 2a). Additionally, the decrease in the NPQ value in the absence of Fe with Se indicates that less excess excitation energy was generated in this treatment (Fig. 3f), reducing the risk of damage to the photosystem.

The absence of Fe can cause significant changes in plant metabolites, such as sugars, amino acids, and secondary metabolites, impacting the plant's life cycle (Zhang et al. 2019). In the present study, an increase in sucrose and starch concentrations were observed, particularly in the absence of Se (Fig. 4c–d and S1). However, sugars, such as glucose and fructose, and organic acids, such as fumarate and malate, were not affected by the imposition of treatments. (Fig. 4a–b, e–f). Sucrose and starch are carbohydrates produced from photosynthesis (Zargar et al. 2015); therefore, as there was limited plant development when plants were exposed to the absence of Fe without Se (Fig. 1a, d), the accumulation these compounds likely occurred due to reduced sink demand (Thalmann and Santelía, 2017). Results consistent with ours were found in soybean (Chu et al. 2019) and cucumber (De Nisi et al. 2012). Furthermore, the accumulation of end products of photosynthesis can result in retroinhibition of the photosynthetic process (Zargar et al. 2015), further contributing to the reduction in *A*, which can lead to the overproduction of reactive oxygen species (ROS), as verified by Lapaz et al. (2023). On the other hand, these responses were less pronounced in plants exposed to the absence of Fe with Se. These findings indicate that Se has the ability to modulate photosynthetic metabolism (Cunha et al. 2022; Cunha et al. 2023).

The reduction in total protein concentration and the increase in total amino acid concentration in soybean plants exposed to the absence of Fe without Se (Fig. 5a–b) may be related to protein

degradation, as previously reported in soybean plants involving the degradation of proteins in the multiprotein thylakoid complex (Muneer and Jeong, 2015). Furthermore, the decrease in ammonia concentration (Fig. 5d) suggests limitations in the assimilation steps of nitrogen into glutamate, as nitrate reductase (NR), nitrite reductase (NiR), and glutamate synthase (GOGAT) require Fe as a Fe–heme group or Fe–S cluster (Borlotti et al. 2012; Li et al. 2021). In this context, as there was protein degradation, it is also possible that plants may be using non-essential proteins as a source of amino acids. Parallel to this, the translocation of amino acids from the root to the shoot may have potentiated the total amino acid concentration (Borlotti et al. 2012), mainly in the absence of Fe with Se, since the protein degradation was attenuated in this treatment.

Just like the observed increase in total amino acid concentration, the proline concentration also increased in the absence of Fe (Fig. 5c). In a study conducted with six barley varieties exposed to Fe deficiency, it was observed that proline increased in the leaves (Arias-Baldrich et al. 2015). Furthermore, it has been proposed that the accumulation of proline in the shoot of rice can help alleviate the reduction of mitochondrial electron transport caused by this micronutrient deficiency (AliaSaradhi 1993). These findings reinforce the importance of proline for plants under Fe-deficient conditions.

5. Conclusion

In the absence of Fe, plants treated with Se exhibited positive modulation in *A*, EiC, and photochemical traits compared to plants without Se. The synergistic absence of Se and Fe compromised shoot and root dry mass and protein concentration. Thus, the supply of Se, in the absence or presence of Fe, showed beneficial effects in alleviating the negative effects of Fe deficiency in soybean plants. These findings highlight the potential of Se as a valuable intervention to mitigate Fe deficiency in soybean crops.

References

AliaSaradhi, P. P. (1993). Suppression in mitochondrial electron transport is the prime cause behind stress-induced proline accumulation. Biochemical and Biophysical Research Communications, 193(1), 54-58. https://doi.org/10.1006/bbrc.1993.1589

Álvarez-Fernández, A., Melgar, J. C., Abadía, J., Abadía, A. (2011). Effects of moderate and severe iron deficiency chlorosis on fruit yield, appearance and composition in pear (*Pyrus communis* L.) and peach (*Prunus persica* (L.) Batsch). Environmental and Experimental Botany, 71(2), 280-286. https://doi.org/10.1016/j.envexpbot.2010.12.012

Arias-Baldrich, C., Bosch, N., Begines, D., Feria, A. B., Monreal, J. A., García-Mauriño, S. (2015). Proline synthesis in barley under iron deficiency and salinity. Journal of Plant physiology, 183, 121-129. https://doi.org/10.1016/j.jplph.2015.05.016

Borlotti, A., Vigani, G., Zocchi, G. (2012). Iron deficiency affects nitrogen metabolism in cucumber (*Cucumis sativus* L.) plants. BMC Plant Biology, 12(1), 1-15. https://doi.org/10.1186/1471-2229-12-189

Bradford, M. M. (1976). A rapid and sensitive method for the quantitation of microgram quantities of protein utilizing the principle of protein-dye binding. Analytical biochemistry, 72(1-2), 248-254. https://doi.org/10.1016/0003-2697(76)90527-3

Carillo, P., Gibon, Y. (2011). Protocol: Extraction and determination of proline. PrometheusWiki, 2011, 1-5.

Chu, Q., Sha, Z., Maruyama, H., Yang, L., Pan, G., Xue, L., Watanabe, T. (2019). Metabolic reprogramming in nodules, roots, and leaves of symbiotic soybean in response to iron deficiency. Plant, Cell Environment, 42(11), 3027-3043. https://doi.org/10.1111/pce.13608

Clark, R. B. (1975). Characterization of phosphatase of intact maize roots. Journal of Agricultural and Food Chemistry, 23(3), 458-460. https://doi.org/10.1021/jf60199a002

Cross, J. M., von Korff, M., Altmann, T., Bartzetko, L., Sulpice, R., Gibon, Y., Palacios, N., Stitt, M. (2006). Variation of enzyme activities and metabolite levels in 24 *Arabidopsis* accessions growing in carbon-limited conditions. Plant Physiology, 142(4), 1574-1588. https://doi.org/10.1104/pp.106.086629

Cunha, M. L. O., de Oliveira, L. C. A., Mendes, N. A. C., Silva, V. M., Vicente, E. F., dos Reis, A. R. (2023). Selenium Increases Photosynthetic Pigments, Flavonoid Biosynthesis, Nodulation, and Growth of Soybean Plants (*Glycine max* L.). Journal of Soil Science and Plant Nutrition, 1-11. https://doi.org/10.1007/s42729-023-01131-8

Cunha, M. L. O., de Oliveira, L. C. A., Silva, V. M., Montanha, G. S., dos Reis, A. R. (2022). Selenium increases photosynthetic capacity, daidzein biosynthesis, nodulation and yield of peanuts plants (*Arachis hypogaea* L.). Plant Physiology and Biochemistry, 190, 231-239. https://doi.org/10.1016/j.plaphy.2022.08.006

De Nisi, P., Vigani, G., Dell'Orto, M., Zocchi, G. (2012). Application of the split root technique to study iron uptake in cucumber plants. Plant Physiology and Biochemistry, 57, 168-174. https://doi.org/10.1016/j.plaphy.2012.05.022

dos Santos, L. R., Paula, L. D. S., Pereira, Y. C., da Silva, B. R. S., Batista, B. L., Alsahli, A. A., Lobato, A. K. D. S. (2021). Brassinosteroids-mediated amelioration of iron deficiency in soybean plants: beneficial effects on the nutritional status, photosynthetic pigments and chlorophyll fluorescence. Journal of Plant Growth Regulation, 40, 1803-1823. https://doi.org/10.1007/s00344-020-10232-y

Fernie, A. R., Roscher, A., Ratcliffe, R. G., Kruger, N. J. (2001). Fructose 2,6- biphosphate activates pyrophosphate: fructose-6-phosphate 1-phosphotranferase and increase triose phosphate to hexose phosphate cycling in heterotrophic cells. Plants, 212(2), 250-263. https://doi.org/10.2135/cropsci1971.0011183X001100060051x

Gattullo, C. E., Youry, P. I. I., Allegretta, I., Medici, L., Cesco, S., Mimmo, T., Terzano, R. (2018). Iron mobilization and mineralogical alterations induced by iron-deficient cucumber plants (*Cucumis sativus* L.) in a calcareous soil. Pedosphere, 28(1), 59-69. https://doi.org/10.1016/S1002-0160(15)60104-7

Gonzalo, M.J., Lucena, J.J., Hernández-Apaolaza, L., 2013. Effect of silicon addition on soybean (*Glycine max*) and cucumber (*Cucumis sativus*) plants grown under iron deficiency. Plant Physiol. Biochem., 70, 455–461. https://doi.org/10.1016/j.plaphy.2013.06.007

Hajiboland, R., Sadeghzadeh, N., Bosnic, D., Bosnic, P., Tolrà, R., Poschenrieder, C., Nikolic, M. (2020). Selenium activates components of iron acquisition machinery in oilseed rape roots. Plant and Soil, 452, 569-586. https://doi.org/10.1007/s11104-020-04599-w

Hantzis, L. J., Kroh, G. E., Jahn, C. E., Cantrell, M., Peers, G., Pilon, M., Ravet, K. (2018). A program for iron economy during deficiency targets specific Fe proteins. Plant Physiology, 176(1), 596-610. https://doi.org/10.1104/pp.17.01497

Haque, A. M., Rahman, M. A., Das, U., Rahman, M. M., Elseehy, M. M., El-Shehawi, A. M., Parvez, M. S., Kabir, A. H. (2022). Changes in physiological responses and MTP (metal tolerance protein) transcripts in soybean (*Glycine max*) exposed to differential iron availability. Plant Physiology and Biochemistry, 179, 1-9. https://doi.org/10.1016/j.plaphy.2022.03.007

He, X. L., Zhang, W. Q., Zhang, N. N., Wen, S. M., Chen, J. (2023). Hydrogen sulfide and nitric oxide regulate the adaptation to iron deficiency through affecting Fe homeostasis and thiol redox modification in *Glycine max* seedlings. Plant Physiology and Biochemistry, 194, 1-14. https://doi.org/10.1016/j.plaphy.2022.11.003

Ibañez, T. B., Santos, L. F. D. M., Lapaz, A. D. M., Ribeiro, I. V., Ribeiro, F. V., Reis, A. R. D., Moreira, A., Heinrichs, R. (2020). Sulfur modulates yield and storage proteins in soybean grains. Scientia Agricola, 78. https://doi.org/10.1590/1678-992X-2019-0020

Kaya, C., Ashraf, M., 2019. The mechanism of hydrogen sulfide mitigation of iron deficiency-induced chlorosis in strawberry (*Fragaria* × *ananassa*) plants. Protoplasma 256, 371–382. https://doi.org/10.1007/s00709-018-1298-x

Kobayashi, T., Nozoye, T., Nishizawa, N. K. (2019). Iron transport and its regulation in plants. *Free Radical Biology and Medicine*, 133, 11-20. https://doi.org/10.1016/j.freeradbiomed.2018.10.439

Kroh, G. E., Pilon, M. (2020). Regulation of iron homeostasis and use in chloroplasts. International Journal of Molecular Sciences, 21(9), 3395. https://doi.org/10.3390/ijms21093395

Lapaz, A. M., Yoshida, C. H. P., Gorni, P. H., Freitas-Silva, L. D., Araújo, T. D. O., Ribeiro, C. (2022). Iron toxicity: effects on the plants and detoxification strategies. Acta Botanica Brasilica, 36. https://doi.org/10.1590/0102-33062021abb0131

Lapaz, A. M., Yoshida, C. H. P., Vieira, J. G., Silva, J. N. B., Dal-Bianco, M., Ribeiro, C. (2023). Promising role of selenium in mitigating the negative effects of iron deficiency in soybean leaves. Environmental and Experimental Botany, 105356. https://doi.org/10.1016/j.envexpbot.2023.105356

Lei, G. J., Zhu, X. F., Wang, Z. W., Dong, F., Dong, N. Y., Zheng, S. J. (2014). Abscisic acid alleviates iron deficiency by promoting root iron reutilization and transport from root to shoot in *Arabidopsis*. Plant, cell environment, 37(4), 852-863. https://doi.org/10.1111/pce.12203

Li, J., Cao, X., Jia, X., Liu, L., Cao, H., Qin, W., Li, M. (2021). Iron deficiency leads to chlorosis through impacting chlorophyll synthesis and nitrogen metabolism in *Areca catechu* L. Frontiers in Plant Science, 12, 710093. https://doi.org/10.3389/fpls.2021.710093

Lisec, J., Schauer, N., Kopka, J., Willmitzer, L., Fernie, A. R. (2006). Gas chromatography mass spectrometry–based metabolite profiling in plants. Nature protocols, 1(1), 387. https://doi.org/10.1038/nprot.2006.59

Maxwell, K., Johnson, G. N. (2000). Chlorophyll fluorescence—a practical guide. Journal of experimental botany, 51(345), 659-668. https://doi.org/10.1093/jexbot/51.345.659

McCullough, H. (1967). The determination of ammonia in whole blood by a direct colorimetric method. Clínica chimica acta, 17(2), 297-304.https://doi.org/10.1016/0009-8981(67)90133-7

Muneer, S., Jeong, B. R. (2015). Silicon decreases Fe deficiency responses by improving photosynthesis and maintaining composition of thylakoid multiprotein complex proteins in soybean plants (*Glycine max* L.). Journal of plant growth regulation, 34, 485-498. https://doi.org/10.1007/s00344-015-9484-y

Nunes-Nesi, A., Carrari, F., Gibon, Y., Sulpice, R., Lytovchenko, A., Fisahn, J., Graham, J., Ratcliffe, R. G., Sweetlove, L. J., Fernie, A. R. (2007). Deficiency of mitochondrial fumarase activity in tomato plants impairs photosynthesis via an effect on stomatal function. The Plant Journal 50, 1093-1106. https://doi.org/10.1111/j.1365-313X.2007.03115.x

Peña Calzada, K., Olivera Viciedo, D., Habermann, E., Calero Hurtado, A., Lupino Gratão, P., De Mello Prado, R., Lata-Tenesaca, L. F., Martinez, C. A., Celi, G. E. A., Rodríguez, J. C. (2022). Exogenous application of amino acids mitigates the deleterious effects of salt stress on soybean plants. Agronomy, 12(9), 2014. https://doi.org/10.3390/agronomy12092014

R Core Team. R: A language and environment for statistical computing. R Foundation for Statistical Computing, Vienna, Austria. 2019. Disponível em: https://www.R-project.org/

Rahman, M. A., Bagchi, R., El-Shehawi, A. M., Elseehy, M. M., Anee, S. A., Lee, K. W., Kabir, A. H. (2022). Physiological and molecular characterization of strategy-I responses and expression of Fe-transporters in Fe-deficient soybean. South African Journal of Botany, 147, 942-950. https://doi.org/10.1016/j.sajb.2022.03.052

Sarruge, J. R., HAAG, H. P. (1974). Análises químicas em plantas (p. 56). Piracicaba: Esalq.

Solti, Á., Kovács, K., Basa, B., Vértes, A., Sárvári, É., Fodor, F. (2012). Uptake and incorporation of iron in sugar beet chloroplasts. Plant Physiology and Biochemistry, 52, 91-97. https://doi.org/10.1016/j.plaphy.2011.11.010

Terry, N., Low, G. (1982). Leaf chlorophyll content and its relation to the intracellular localization of iron. Journal of Plant Nutrition, 5(4-7), 301-310. https://doi.org/10.1080/01904168209362959

Thalmann, M., Santelia, D. (2017). Starch as a determinant of plant fitness under abiotic stress. New Phytologist, 214(3), 943-951. https://doi.org/10.1111/nph.14491

Toral-Juárez, M. A., Avila, R. T., Cardoso, A. A., Brito, F. A., Machado, K. L., Almeida, W. L., Souza, R. P. B., Martins, C.V. S., DaMatta, F. M. (2021). Drought-tolerant coffee plants display increased tolerance to waterlogging and post-waterlogging reoxygenation. Environmental and Experimental Botany, 182, 104311. https://doi.org/10.1016/j.envexpbot.2020.104311

Wang, Y., Xu, C., Li, K., Cai, X., Wu, M., Chen, G. (2017). Fe deficiency induced changes in rice (*Oryza sativa* L.) thylakoids. Environmental Science and Pollution Research, 24, 1380-1388. https://doi.org/10.1007/s11356-016-7900-x

Yin, H., Qi, Z., Li, M., Ahammed, G. J., Chu, X., Zhou, J. (2019). Selenium forms and methods of application differentially modulate plant growth, photosynthesis, stress tolerance, selenium content and speciation in *Oryza sativa* L. Ecotoxicology and environmental safety, 169, 911-917. https://doi.org/10.1016/j.ecoenv.2018.11.080

Zargar, S. M., Agrawal, G. K., Rakwal, R., Fukao, Y. (2015). Quantitative proteomics reveals role of sugar in decreasing photosynthetic activity due to Fe deficiency. Frontiers in Plant Science, 6, 592. https://doi.org/10.3389/fpls.2015.00592

Zhang, X. Y., Jia, X. M., Zhang, R., Zhu, Z. L., Liu, B., Gao, L. Y., Wang, Y. X. (2019). Metabolic analysis in *Malus halliana* leaves in response to iron deficiency. Scientia Horticulturae, 258, 108792. https://doi.org/10.1016/j.scienta.2019.108792

Material supplementary

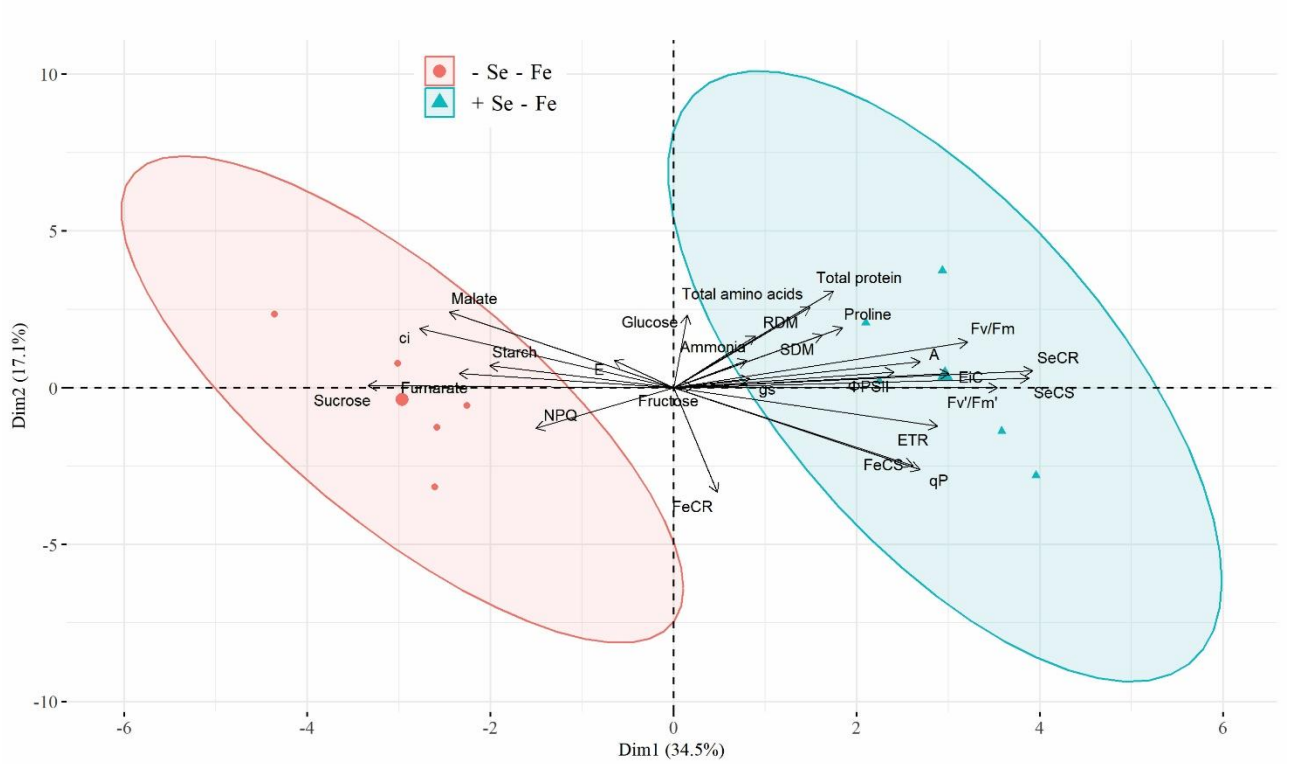

Figure S1. Biplot component analysis in soybean plants at the V3 phenological stage exposed to the nutrient solution with absence (–Fe) for 9 days, associated with the absence (0 µM) or presence of sodium selenate (10 µM), with the beginning of the Se supply 3 days before the imposition of Fe deficiency Shoot dry mass (SDM), root dry mass (RDM), iron concentration in the shoot (FeCS), iron concentration in the root (FeCR), selenium concentration in the shoot (SeCS), selenium concentration in the root (SeCR), net photosynthetic rate (A), stomatal conductance (g_s), transpiration rate (E), intercellular CO_2 concentration (Ci), carboxylation efficiency (EiC), maximum efficiency of PSII photochemistry (F_v/F_m), excitation energy capture efficiency of PSII reaction centers (F_v'/F_m'), effective PSII quantum yield (Φ_{PSII}), electron transport rate (ETR), photochemical quenching (q_P), and non-photochemical quenching (NPQ).